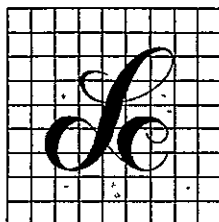
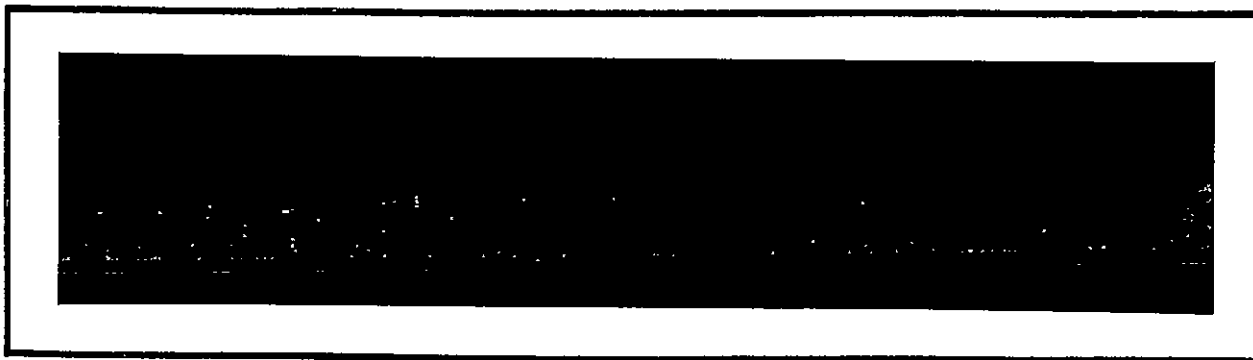


NASA CR-

160538



LinCom Corporation

PO Box 2793D, Pasadena, Calif 91105

LinCom

FINAL REPORT

(NASA-CR-160538) ANALYTICAL SIMULATION OF
SPS SYSTEM PERFORMANCE, VOLUME 3, PHASE 3
Final Report (LinCom Corp., Pasadena,
Calif.) 91 p HC A05/MF A01

N80-18566

CSCL 10B

Unclas

63/44 47387

ANALYTICAL SIMULATION OF
SPS SYSTEM PERFORMANCE
VOLUME III

PREPARED FOR

NASA JOHNSON SPACE CENTER
HOUSTON, TX 77058

TECHNICAL MONITOR: JACK SEYL

CONTRACT No. NAS9-15782

PREPARED BY

A. V. KANTAK
W. C. LINDSEY

LINCOM CORPORATION
P.O. BOX 2793D
PASADENA, CA 91105

JANUARY 1980

TR-0180-0779

LinCom

ACKNOWLEDGEMENT

The authors wish to acknowledge the discussions held with Mr. Jack Seyl and Dr. G. D. Arndt of the Johnson Space Center and for providing us with various articles of interest. In addition, the support and encouragement of Mr. R. H. Dietz and Mr. R. O. Piland of the Johnson Space Center is greatly appreciated.

TABLE OF CONTENTS

	PAGE
1.0 INTRODUCTION	1
2.0 DESCRIPTION OF SPS ANTENNA SIMULATION MODEL AND SYSTEM IMPERFECTIONS	3
2.1 Antenna Structure and Mechanical System Imperfections	3
2.2 Electrical System Imperfections	8
3.0 SPS POWER TRANSFER EFFICIENCY	10
3.1 Averaged Power Pattern	10
3.2 Power Transfer Efficiency	14
3.3 Computation of Efficiency	16
3.4 Effects of System Jitters and Imperfections on the Power Transfer Efficiency of the Spacetenna	17
4.0 EFFECTS OF ANTENNA SYSTEM IMPERFECTIONS ON THE SPACETENNA POWER PATTERN	26
4.1 Effects of Antenna System Imperfections on the Power Density at the Rectenna	32
5.0 EFFECT OF SYSTEM IMPERFECTIONS ON THE MAIN BEAM GAIN LOSS	38
5.1 Effect of Electrical System Imperfections on the Main Beam Gain Loss	38
5.2 Effects of Mechanical System Imperfections on the Loss of Gain	43
6.0 EFFECTS OF SYSTEM IMPERFECTIONS ON THE POINTING ERROR	46
REFERENCES	51
APPENDIX. PROGRAM STATUS	52
I. SOLARSIM SPS System Definition and Computational Considerations	52
II. SOLARSIM Subroutine POINTING ERROR	61
III. SOLARSIM Subroutine VARSUB	63

TABLE OF CONTENTS (Cont'd)

	PAGE
IV. SOLARSIM Subroutine POWER PATTERN	69
V. SOLARSIM Subroutine POWER TRANSFER EFFICIENCY	72

1.0 INTRODUCTION

The spacetenna is configured to be a circular disk of 1 Km diameter having 101,552 microwave tubes (power amplifiers) designed to focus and point the phase coherent microwave beam to a ground based rectifying antenna (rectenna) which is about 10 Km in diameter. The focusing of the microwave beam is based upon the retrodirective active phased array concept which uses the conjugated phase of an uplink pilot wave from the rectenna center. The spacetenna power transmission system consists of three major systems: (1) the solar power to electrical power conversion system, (2) the reference phase distribution system and (3) the beam forming and microwave power generating system.

The last two systems were described in great detail in previous reports [1-3], currently we shall be concerned with establishing the far-field performance associated with the reference phase distribution system and the beam forming and microwave power generating system. The major technique used in the performance evaluation is that of analytical simulation, i.e., a combination of analysis and computer simulation. The far-field pattern produced by the spacetenna is affected not only by the systematics and the random effects introduced by the above two systems (electrical system) but also by the systematics and the random effects introduced by the spacetenna mechanical construction such as subarray tilts and jitters (mechanical system). Thus all the performance measures are functions of the systematics and randomness introduced by the electrical as well as mechanical systems of the spacetenna. These electrical and mechanical system imperfections are listed below:

- a. Electrical System Imperfections:
 1. Phase jitter introduced by the reference phase distribution system.
 2. Current amplitude jitter introduced by the power amplifiers.
 3. Instabilities introduced by the power transponder into the outgoing power wave phase.
- b. Mechanical System Imperfections:
 1. Mean mechanical tilt of the subarrays (mechanical pointing error).
 2. Jitter on the tilt of the subarrays.
 3. Location jitters of the radiating elements.
 4. Location jitters of the pilot receiving element.

It should be noted that all these jitters are spatial jitters. All these mechanical and electrical imperfections have degrading effects on SPS performance parameters. These performance parameters can be grouped as follows:

1. Power Transfer Efficiency
2. Pointing Error
3. Main Beam Gain Loss
4. Side Lobe Levels
5. Grating Lobes

This report is organized as follows: Section 2 is devoted to a description of the simulation model for the SPS spacetenna and the associated system imperfections. In the next section, we address the key performance issue involved with the SPS--the overall power transfer efficiency as a function of the system imperfections. To complete our

analysis, the subsequent sections are devoted to other specialized system performance measures. They include: average power pattern (Section 4), mean beam gain reduction (Section 5) and pointing error (Section 6). The SOLARSIM subroutines and a user guide with sample runs are documented in the Appendix.

2.0 DESCRIPTION OF SPS ANTENNA SIMULATION MODEL AND SYSTEM IMPERFECTIONS

2.1 Antenna Structure and Mechanical System Imperfections

The mechanical imperfections can be applied to two different entities: the radiating elements and the conjugating elements. To understand the mechanical system imperfections, we describe the antenna system as follows.

The 10 dB power taper in the present baseline is achieved by dividing the spacetenna into 10 distinct power density rings. A quadrant of the spacetenna is shown in Fig.2.1. The radii of these rings run from about 94 meters to a maximum of 500 meters as shown. The power density per ring is varied by changing the number of PAs feeding per unit radiating surface. For example, the number of power amplifiers (PA) feeding a 10.4m x 10.4m square of slotted waveguide changes from 36 to 4 from the innermost to the outermost ring. The power taper from the spacetenna center to its edge is thus 9.5 dB to be exact.

The reference system assumes that phase conjugation is performed on each PA that feeds a subarray. By a subarray we mean a planar group of slotted waveguides in the center of which phase conjugation is performed. Hence only the central radiating element is truly retrodirective. The other elements on the same subarray will experience differential phase shifts defined by the projections of the location of the elements along the boresight. The size of subarray in the baseline

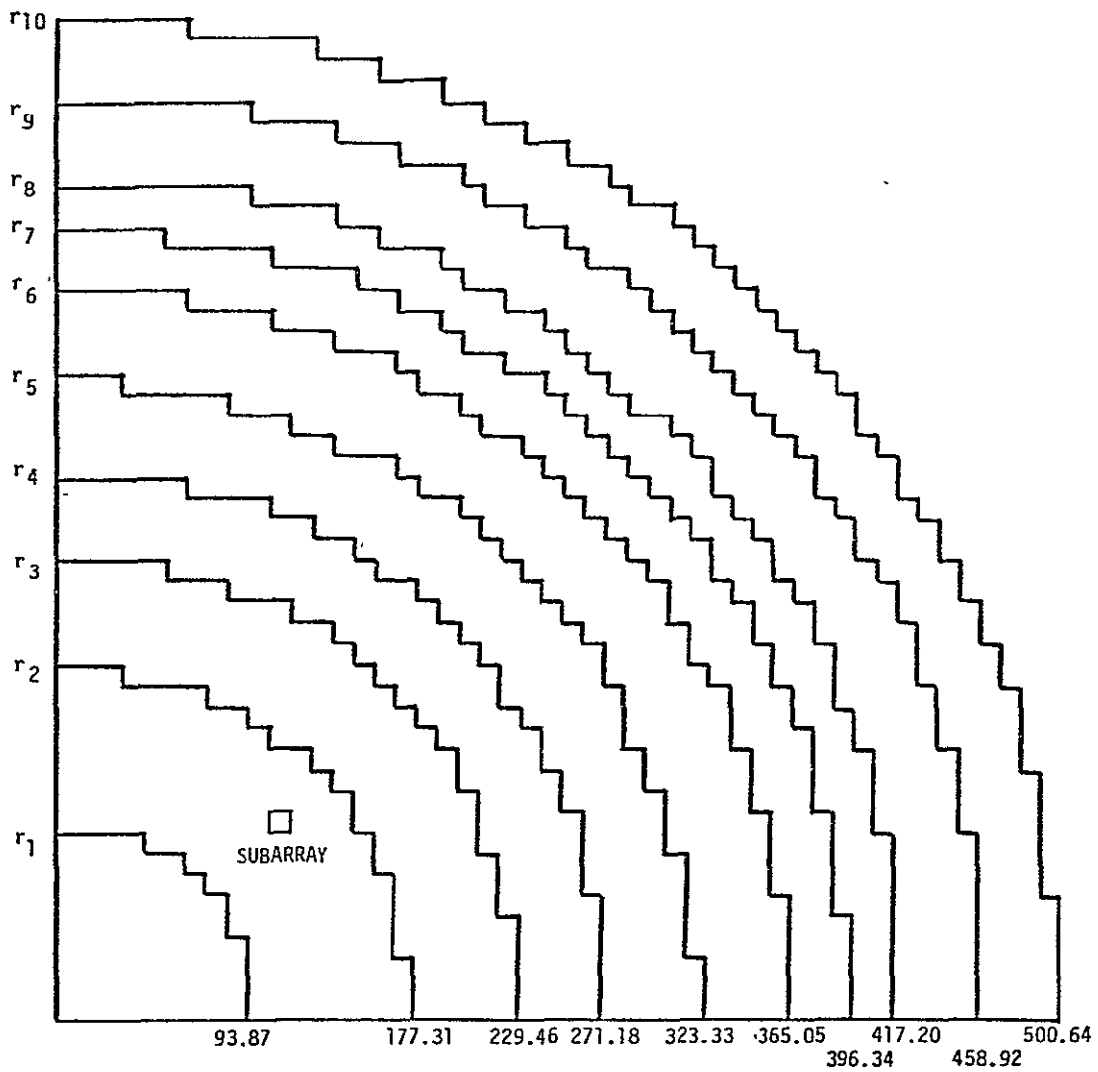


Figure 2.1. Spacetenna Power Density Rings.

80 0061

varies from $1.73 \times 1.73 \text{ m}^2$ to $5.2 \times 5.2 \text{ m}^2$ from the center to the edge of the spacetenna. The details are given in Fig. 2.2. Also shown in the same figure is the fixed size subarray geometry conceived by Boeing. In that configuration all subarrays have a fixed size of $10.4 \times 10.4 \text{ m}^2$. Only one conjugation center is provided on each subarray.

For a perfectly flat spacetenna, the normal directions of each subarray are all identical, i.e., they all coincide with the normal direction of the spacetenna as a whole. Since the spacetenna is never perfectly flat in reality, each subarray will point in a different direction. For SOLARSIM, we adopt the subarray tilt model depicted in Fig. 2.3. The dashed line shows the ideal position of the subarray. With tilts, the subarray is depicted by the solid line. Note that the tilted subarray makes an angle θ_x with the axis and angle θ_y with the y axis. The angle between the present normal direction and the ideal direction is given by $\theta^2 = \theta_x^2 + \theta_y^2$. The tilt angles θ_x and θ_y have mean components denoted by $E(\theta_x)$ and $E(\theta_y)$. They represent the errors in the SPS steering mechanism made in pointing the spacetenna towards the rectenna center. The mean values $E(\theta_x)$ and $E(\theta_y)$ are the same for all the subarrays and they are referred to as the mechanical pointing error in the x- and y-direction. The perturbation about these means, i.e., $\theta_x - E(\theta_x)$ and $\theta_y - E(\theta_y)$ represent the variations of the tilt angles from one subarray to another. They are assumed to be Gaussian with variances σ_{θ_x} and σ_{θ_y} .

In the above model, we have modeled the subarrays to be flat surfaces. This assumption is justifiable since we are only interested in the global behavior of the subarray. However, when we are concerned with the radiating elements, we need a more refined model for

FIXED SIZE SUBARRAYS

VARIABLE SIZE SUBARRAYS

POWER DENSITY STEP	NUMBER OF SUBARRAYS	NUMBER OF POWER MODULES PER CONJUGATION PT.	TOTAL # OF POWER MODULES PER DENSITY STEP	POWER DENSITY STEP	SIZE OF SUBARRAY	NUMBER OF SUBARRAYS	TOTAL # OF POWER MODULES PER CONJUGATION POINT	# OF POWER MODULES
1	276	36	9936	1	1.73m x 1.73m	9936	1	9936
2	632	30	18960	2	1.89m x 1.89m	18960	1	18960
3	644	24	15456	3	2.12m x 2.12m	15456	1	15456
4	628	20	12560	4	2.32m x 2.32m	12560	1	12560
5	784	16	12544	5	2.6m x 2.6m	12544	1	12544
6	900	12	10800	6	3m x 3m	10800	1	10800
7	664	9	5976	7	3.46m x 3.46m	5976	1	5976
8	612	8	4896	8	3.67m x 3.67m	4896	1	4896
9	1052	6	6312	9	4.24m x 4.24m	6312	1	6312
10	1028	4	4112	10	5.2m x 5.2m	4112	1	4112
TOTAL FOR FULL ARRAY		7220	101552			101552		101552

SIZE OF THE SUBARRAY = 10.4m x 10.4m

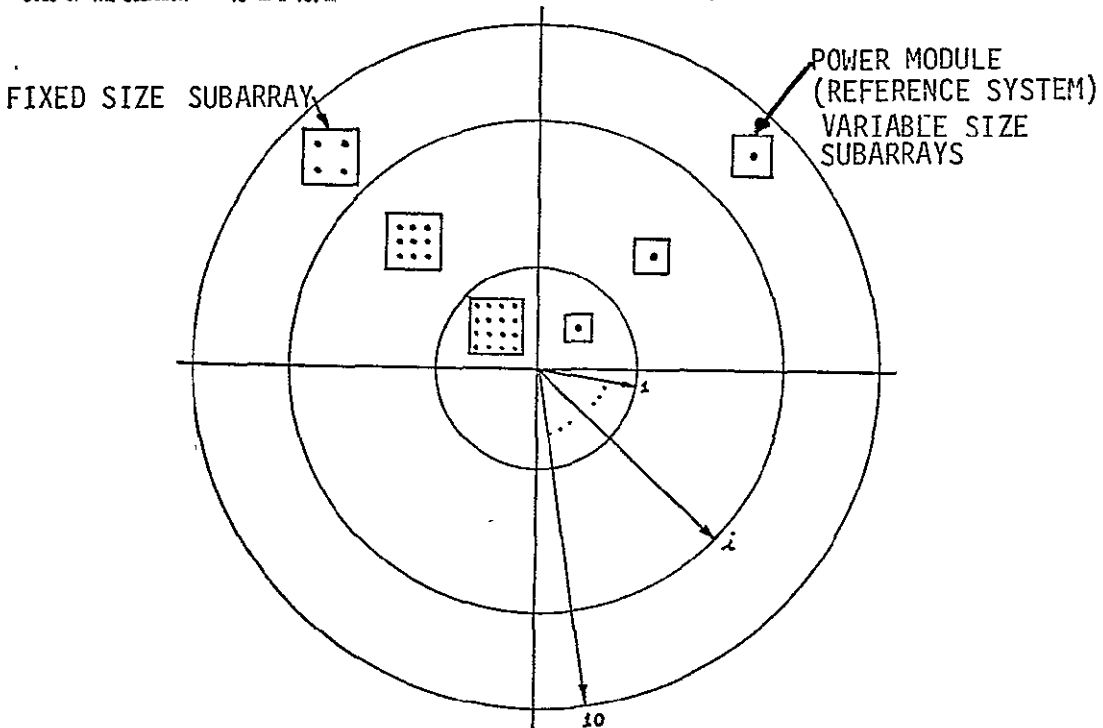


Figure 2.2. Variable and Fixed Size Subarray Geometry.

80 0062

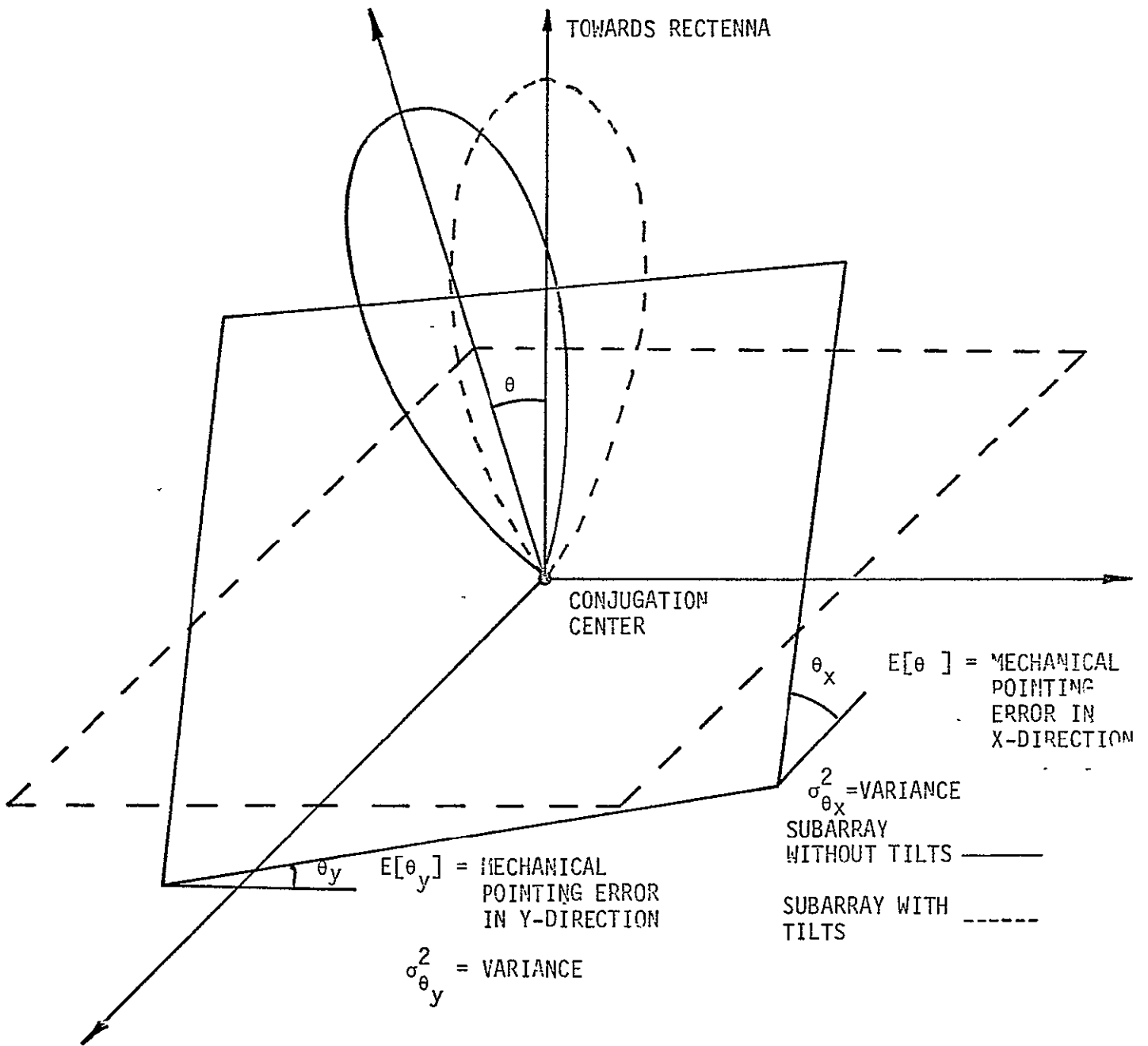


Figure 2.3. Effect of Subarray Mean Tilt and Jitter.

SOLARSIM. Figure 2.4 defines the location uncertainty of the radiating elements and the conjugation point primarily resulting from the unevenness of the subarray surface. The average plane through the subarray defined the ideal subarray used to model the tilt effects. However, the actual locations of the radiating elements and the conjugation point will be perturbed from the average plane. A cross section of a typical subarray surface running through the conjugation point parallel to the y-axis is shown in Fig. 2.4. The location jitter is defined to be the projection of the location of a point along the line joining the ideal center of the subarray and the center of the rectenna.

2.2 Electrical System Imperfections

As mentioned earlier, there are three different sources for electrical imperfection: the phase jitter introduced by the phase distribution system, the phase jitter introduced by the transponder circuitry and the amplitude and phase jitter introduced by the power amplifier. We will discuss only the phase jitter introduced by the phase distribution system because the remaining two cases can be covered by special cases of the first. SOLARSIM has been developed to cover these cases.

The current reference phase distribution tree consists of a four level tree having a branching scheme represented as $16 \times 16 \times 16 \times 25$, i.e., every node on the first level has 16 branches, every node on the second level has 16 branches, every node on the third level has 16 branches and finally every node on the fourth level has 25 branches. This makes a total of 102,400 nodes at the end of the fourth level. The phase is sent from one level to the other by the use of MSRTS (described in

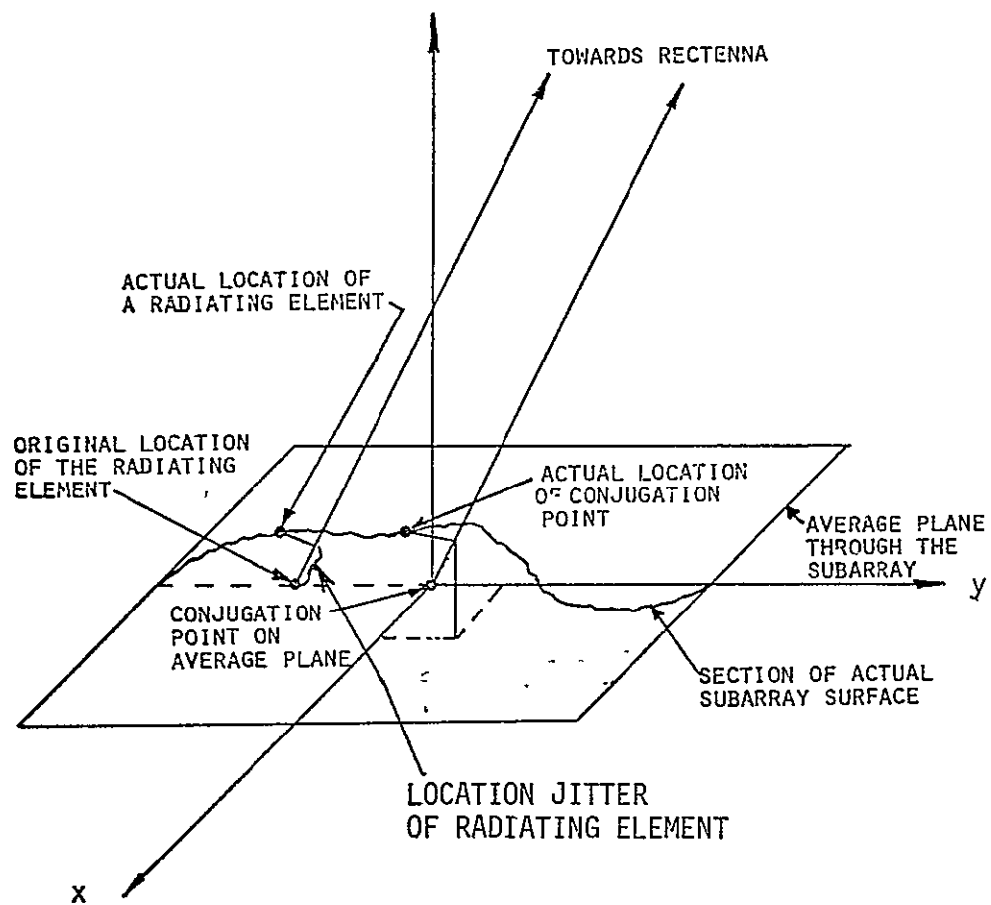


Figure 2.4. Jitters Added Due to Location Uncertainty of Radiating and Conjugation Points.

80 0064

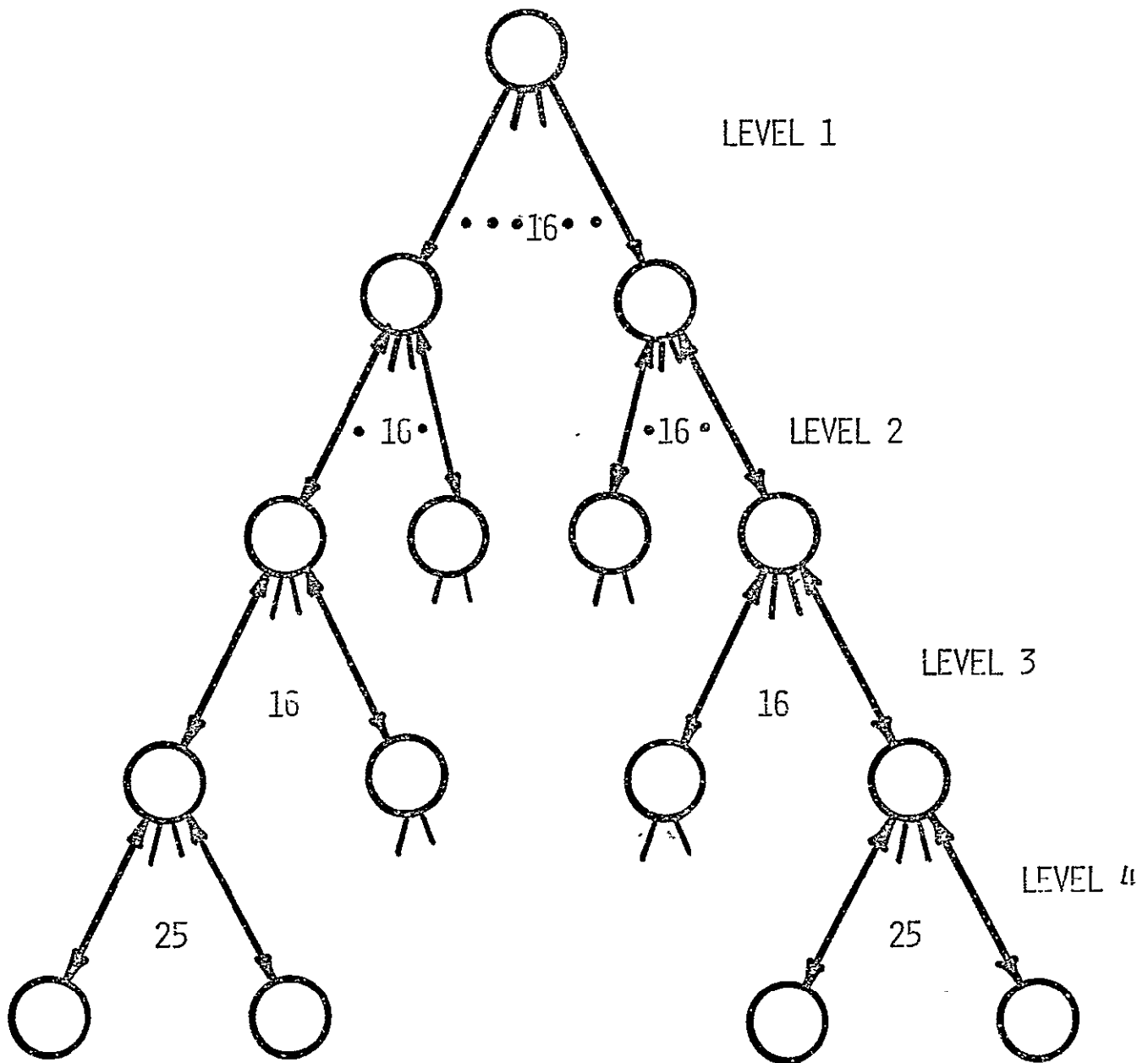
detail in previous reports) and the circuitry, not being perfect, adds phase noise at each level of the phase distribution tree. The phase noise introduced by the transponder circuitry and the power amplifier may be added to the phase noise of the fourth level. The phase distribution tree is shown in Fig. 2.5. In addition, the amplitude variations on the Power Amplifiers must be considered as a random parameter.

3.0 SPS POWER TRANSFER EFFICIENCY

3.1 Averaged Power Pattern

The first step in obtaining the power transfer efficiency of an antenna is to obtain its averaged power pattern including all the random effects. The spacetenna is assumed to be a stepped approximation to a circle of diameter 1 Km, having an area of $0.76 \times 10^6 \text{ mt}^2$. This area is subdivided into what are called the subarrays. These subarrays are not of the same size. Each subarray is fed by a single power amplifier and actual radiating elements in the subarrays are the slotted waveguides. Conjugation of the received pilot phase is done at each power amplifier tube with the help of a constant phase supplied by the phase distribution system. This conjugated phase is used to produce retrodirective power wave. As discussed in the preceding section, the radiated power wave has effects introduced by the mechanical system (due to subarray and waveguide layout) and also the effects introduced by the electrical system (due to the constant phase distribution system for conjugation).

Thus each slot radiates a power beam having an amplitude and phase variation depending upon the electrical system imperfections, the mechanical system imperfections and of course the phase supplied by the



- PHASE NOISES ARE CORRELATED
- POWER SPLITTERS, POWER TRANSPONDERS, PHASE TRACKING PLLS, MULTIPLIERS, MICROWAVE HARDWARE COMPONENTS

Figure 2.5. Four Level Phase Distribution Tree.

conjugator to the power amplifier feeding that slot. Hence each slot has a pattern associated with it, and the power pattern of the spacetenna is obtained by summing all the individual patterns produced by the slots. Such a pattern is random because of the randomness introduced by the mechanical and electrical systems. Hence after averaging (statistical averaging) of the power pattern we obtain the averaged power pattern produced by the spacetenna.

The actual radiating elements are the slots cut in the waveguides (slots are separated from each other by a distance of $\lambda/2$, where λ is the wavelength of the waves in the waveguide). The pattern multiplication principle tells us that the radiation pattern of spacetenna is the multiplication of the element pattern of the radiating elements and the array factor (based on the location of the radiating slots) of the antenna. Array factor of the antenna remains the same regardless of the nature of the radiating elements. The array factor of the spacetenna has a very highly peaked mainlobe having a 3 dB beamwidth of a few tenths of a minute of arc which is comparable to the angle subtended by the rectenna at the spacetenna center. The element factor of the slot is so flat around the boresight for several minutes of arc that the region of interest (the 3 dB beamwidth region) this factor could be approximated by a constant. Hence the radiation pattern of the spacetenna in the region of interest, could be approximated by considering isotropically radiating elements instead of the slots. The spacetenna power pattern using the above approximation has two main parts comprising it. One part depends on the direction (θ, ϕ) which will be called the anisotropic term and the other part independent of (θ, ϕ) will be termed the isotropic part, i.e., (see Figure 3.1)

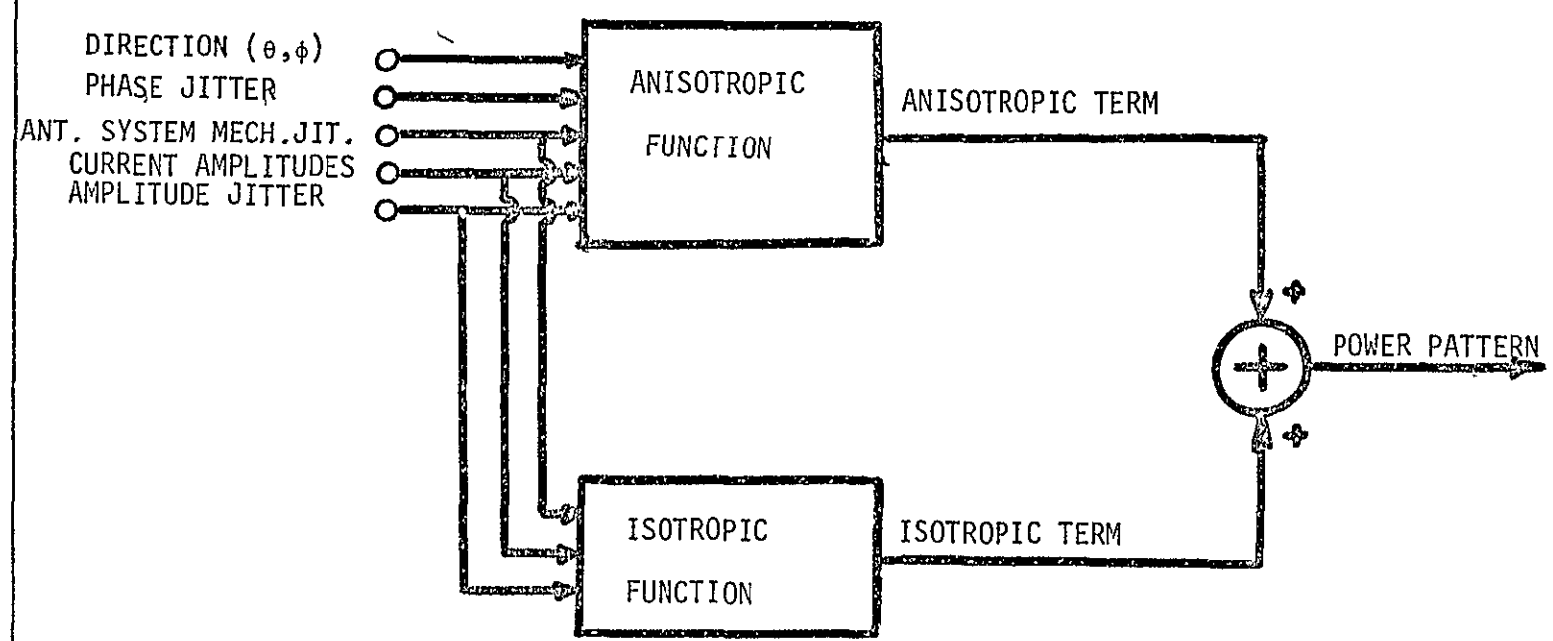


Figure 3-1. Components of the Average Power Pattern.

$$\begin{array}{l} \text{Averaged} \\ \text{Power} \\ \text{Pattern} \end{array} \triangleq E(f f^*) = \text{Anisotropic Term} + \text{Isotropic Term}$$

The spacetenna averaged power pattern takes into account all the system imperfections in the form of jitters. The isotropic term is a function of independent phase disturbances at the slot level. It should be noted that the isotropic term comes into existence only if the phase disturbances at the slot level are statistically independent, e.g., the location jitter on the radiating slots this does not include, for example, the phase disturbance added by the phase distribution system because all the slots in the subarray are affected by the same phase disturbance. One more fact may be pointed out that if the slot element pattern is used in the computation, the only change is that the isotropic term becomes directional due to the element pattern and the total power due to this term reduces by the gain factor (of the slot) from the total power radiated by the isotropic term. A more detailed study of the effects of system imperfections on the average power pattern and power density level will be given in Section 4.0.

3.2 Power Transfer Efficiency

$$\begin{array}{l} \text{POWER TRANSFER} \\ \text{EFFICIENCY} \end{array} = \frac{\text{Power Received by the 10 Km Diameter Rectenna}}{\text{Total Power Radiated by the Spacetenna}} \quad (1)$$

Figure 3.2 makes the idea clear. The power transfer efficiency can be redefined as

$$\begin{array}{l} \text{POWER TRANSFER} \\ \text{EFFICIENCY} \end{array} = \frac{\text{Power Output at Terminals A \& B}}{\text{Power Output at Terminals C \& D}} \quad (2)$$

This definition is convenient because the multiplying constants due to

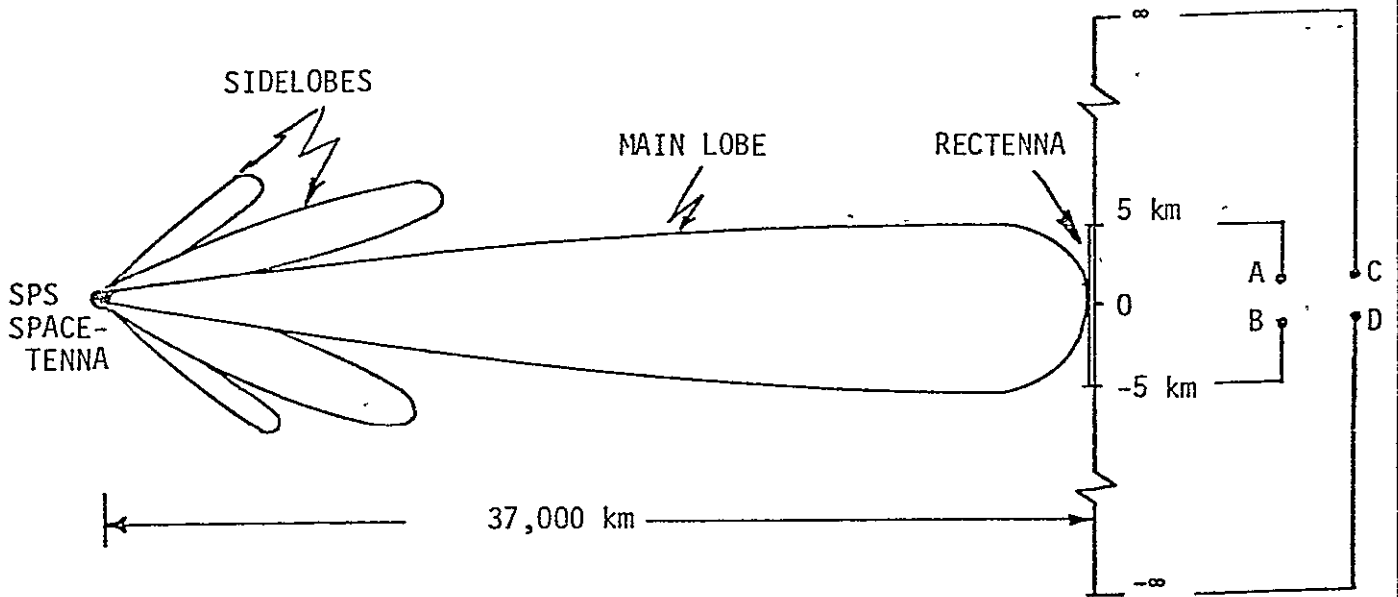


Figure 3.2. Geometry of the Power Pattern.

the propagation through the medium cancel out from the numerator and denominator. The computer program uses this efficiency definition. It may be noticed that the power received by the rectenna as well as the total power radiated by the spacetenna are functions of several parameters such as the spacetenna mechanical pointing error, jitters on the pointing error, jitters on locations of the radiating elements, feed current and phase jitters, to name a few.

3.3 Computation of Efficiency

Computation of total radiated power and the power received by the rectenna is done by integrating the averaged power pattern of the spacetenna over the appropriate regions.

$$\text{TOTAL RADIATED POWER} = \iint_H (\text{averaged power pattern}) \sin \theta d\theta d\phi$$

where the averaged power pattern is obtained as explained in the previous section. Hence

$$\begin{aligned} \text{THE TOTAL RADIATED POWER} &= \iint_H (\text{anisotropic term}) \sin \theta d\theta d\phi \\ &+ \iint_H (\text{isotropic term}) \sin \theta d\theta d\phi \end{aligned}$$

Figure 3.4 shows that the isotropic term is independent of (θ, ϕ) , the direction (that is the reason it is called isotropic). Hence

$$\begin{aligned} \text{TOTAL RADIATED POWER} &= \iint_H (\text{anisotropic term}) \sin \theta d\theta d\phi \\ &+ (\text{isotropic term}) \underbrace{\iint_H \sin \theta d\theta d\phi}_{\text{Constant}} \end{aligned}$$

Similarly,

$$\begin{aligned} \text{RECEIVED POWER} = & \iint_{\theta, \phi \in R} (\text{anisotropic term}) \sin \theta d\theta d\phi \\ & + (\text{isotropic term}) \iint_{\theta, \phi \in R} \sin \theta d\theta d\phi \end{aligned}$$

where R is the region of the rectenna (see Fig. 3.2).

3.4 Effects of System Jitters and Imperfections on the Power Transfer Efficiency of the Spacetenna

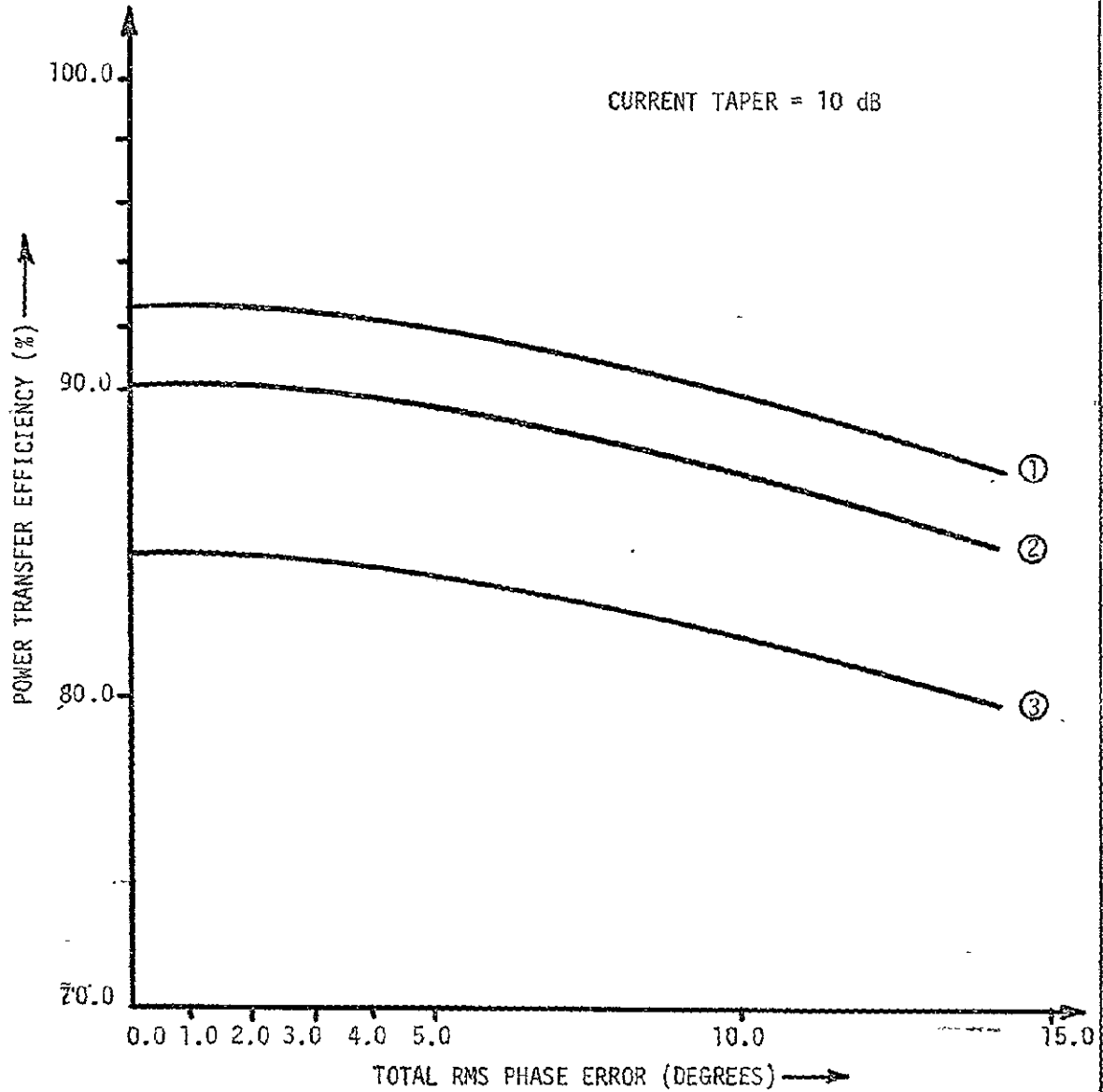
As was done previously, the system jitters and imperfections can be grouped into two main classes, (1) jitters arising due to spacetenna electrical components which includes such effects as the amplitude jitter of the feed currents to the radiating elements of the spacetenna and the phase jitters of the feed currents having their origin at the phase control system required by the phase conjugation scheme, and (2) jitters arising due to the mechanical constructional faults of the spacetenna. This category includes the subarray tilts, tilt jitters and the location jitters. The location jitters basically arise from the misplacement of the radiating elements. As was described earlier, the combined effect of all these disrupting effects is to produce either a pointing error in the main beam pointing or to induce a loss of gain or both. Each of these effects, i.e. the pointing error and the main beam loss, introduces a loss in the power intercepted by the rectenna while the total power radiated by the spacetenna does not alter significantly (except for the amplitude jitter case). This means that the efficiency is a function of the

system jitters and imperfections the sensitivity of the power transfer efficiency to the system jitters is discussed below.

In a previous section the power transfer efficiency was defined. That definition is used to generate results given below. The computer program evaluates the received power as given above, i.e., $\phi_{\epsilon}(0,2\pi)$ and $\theta_{\epsilon}(0,0.464')$. The total radiated power is computed in two parts. For the following results, the first part integrated the anisotropic part of the power pattern over the main lobe and 5 side lobes, i.e. the while space is approximated by $\phi_{\epsilon}(0,2\pi)$ and $\theta_{\epsilon}(0,\text{mainlobe}+5 \text{ side lobes})$. The loss of power resulting by not considering all the side lobes of the pattern is taken care of by multiplying a correction factor. The second part computed the power radiated by the isotropic part of the power pattern. The addition of the two parts produced the total radiated power. The ratio of received power and the total radiated power produced the power transfer efficiency. The systems jitters are the inputs to the program and thus it is possible to investigate the effects of each of the jitters on the power transfer efficiency.

The first set of curves in Fig.3.3 are drawn to investigate the effect of the total phase error added by the phase control system to the outgoing power wave. The power transfer efficiency is plotted against the total phase error with the parameters to be location jitters of the receiving and transmitting elements and the mechanical pointing error with its jitter (subarray tilt and tilt jitter). The first curve of the set is for a spacetenna with no location jitters and no mechanical pointing error or jitter, i.e. this curve is for a mechanically perfect system. In such a case, to have a power transfer efficiency of 90%, the total phase error cannot be allowed to become

Figure 3.3. SPS Power Transfer Efficiency.



LEGEND

- ① MECHANICAL POINTING ERROR (MPE) = 0, LOCATION JITTERS (LJ) = 0
JITTER ON MECHANICAL POINTING = 0
- ② MPE = 10', LJ = 0, JITTER ON MPE = 2'
- ③ MPE = 10', LJ = 2% of λ , JITTER ON MPE = 2'

80 0083

more than 10° at RF or 5° per level of the phase control MSRTS tree structure. The second curve helps to depict the influence of the mechanical pointing error (it is assumed to be $10'$ with a jitter of $2'$) the location jitters are zero in this case. As can be seen from the figure for a total phase error of 10° the power transfer efficiency of the spacetenna drops down to 87.3% and when the location jitters of 2% of λ is added for the transmitting and receiving elements, this number drops down to 82.0%. One may notice from these curves that the power transfer efficiency of the perfect system is about 92.6%. The prime reason for this being that the rectenna intercepts only a part of the mainlobe, i.e., the power in the part of the mainlobe not intercepted by the rectenna and the power in side lobes is lost. This is significant because at the edge of the rectenna the power density is only about 14 dB lower than the power density at the center of the rectenna.

The set of curves in Fig. 3.4 is drawn for a perfect mechanical system, i.e., the location jitters and the mechanical pointing error and the associated jitter are held to zero while the total phase error introduced by the phase control system is the parameter. The current amplitude jitter on the x axis is measured in terms of percent of the nominal value of the current amplitude. As can be seen from the figure, for an amplitude jitter of 5%, the power transfer efficiency of the mechanically perfect spacetenna with the current phase jitter of 0° is 92.3%. This value drops to 91.63 for the total phase error of 5° and to 89.57% for a total phase error of 10° . Fig. 3.5 is a plot for mechanically perfect system with power transfer efficiency versus the total accumulated phase error due to the phase control system

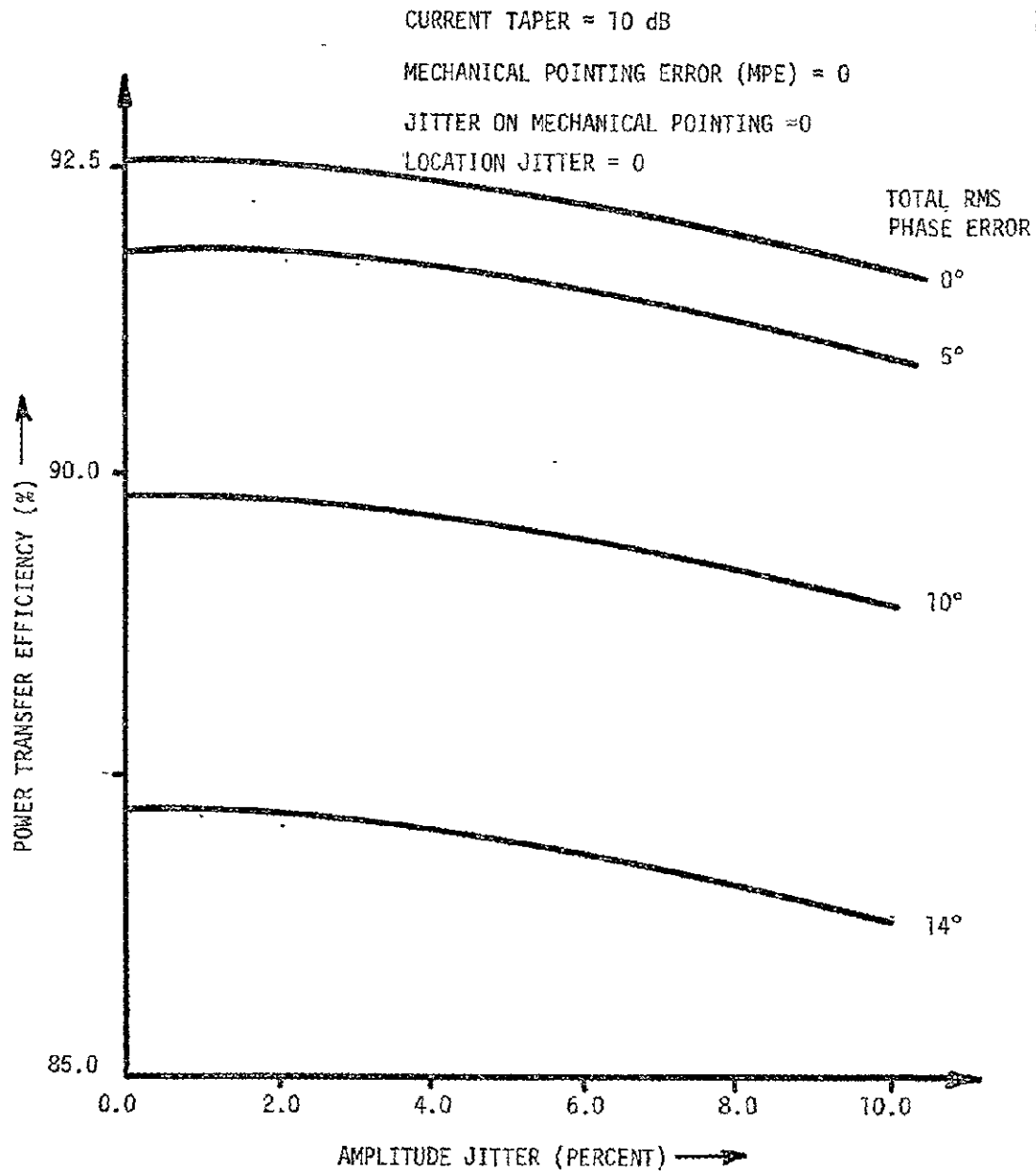


Figure 3.4. Effect of Amplitude Jitter on SPS Power Transfer Efficiency.

80 0084

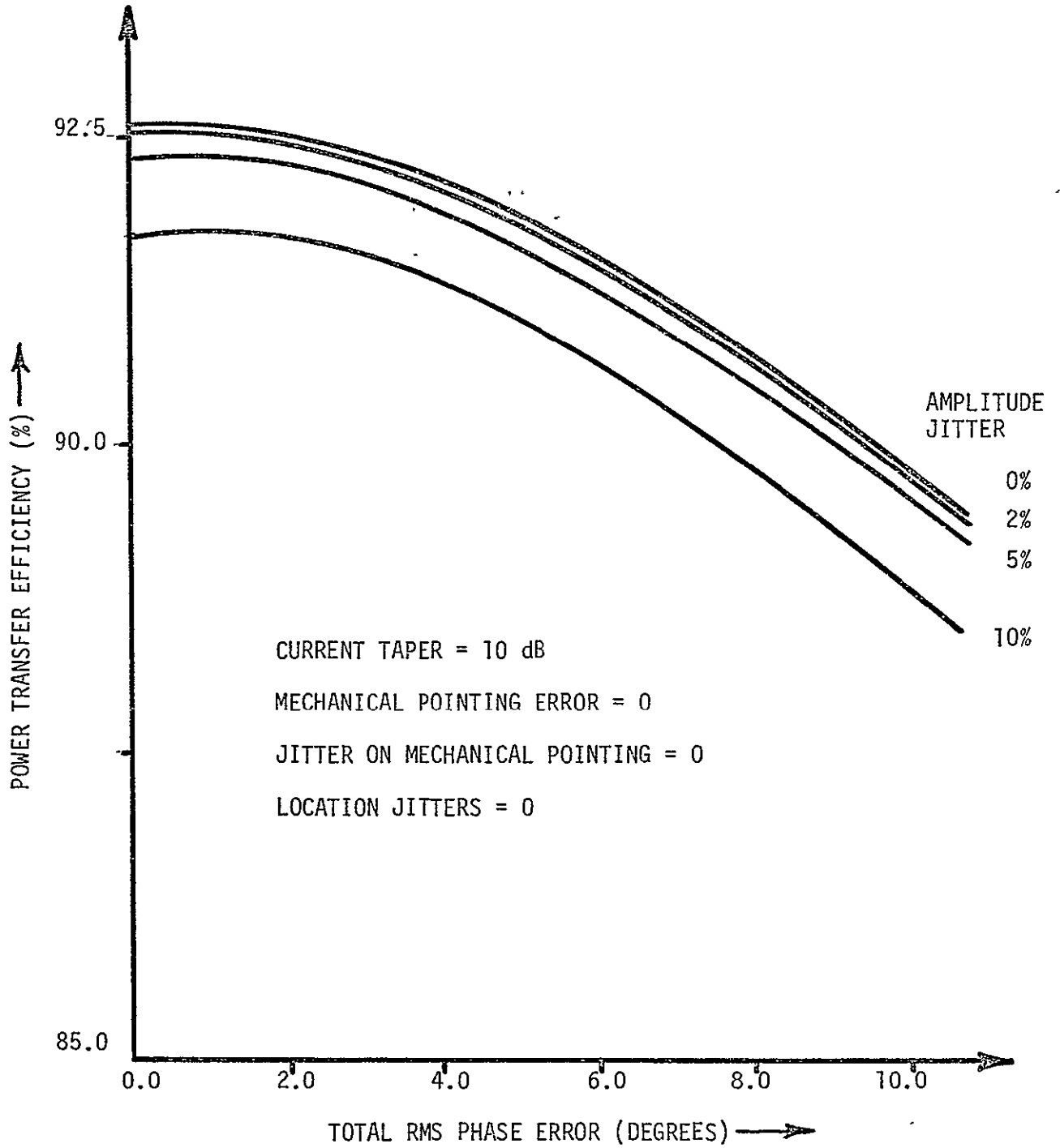


Figure 3.5. Effect of Amplitude Jitter on Power Transfer Efficiency.

80 0085

and the amplitude jitter appears as the parameter for the family of curves. From the last two figures it may be concluded that the power transfer efficiency is relatively insensitive to the amplitude jitters.

The curves in Fig.3.6 and Fig.3.7 are for the investigation of effects of location jitters on the power transfer efficiency. Fig. 3.6 is drawn for the perfect electrical system, i.e. no phase errors and no amplitude jitter also the location jitter of the receiving elements is held to zero. As can be seen from the figure, the degradation of efficiency is rapid. For a location jitter on each radiating element to be $2\% \lambda$ (in the direction of line joining the element and the center of rectenna) the power transfer efficiency drops to 88.3%. As a comparison, the Fig. 3.3 shows that for a phase error of 7° ($2\% \lambda = 7.2^\circ$) the efficiency is down to 91.2%. Fig. 3.7 is drawn for the perfect electrical system and the location jitter on the radiating elements held to zero. It is noticeable that the effect produced by location jitters on the receiving (conjugating) elements is comparable to the effect produced by the phase error. This is true because both these effects enter into the transmission system at the same physical point, i.e., the center of the subarray. One can also say that the location jitter on the receiving elements produce less severe effect on the power transfer efficiency than the location jitter on the radiating elements. These two curves can be used to determine the allowable mechanical tolerances for the construction of the spacetenna.

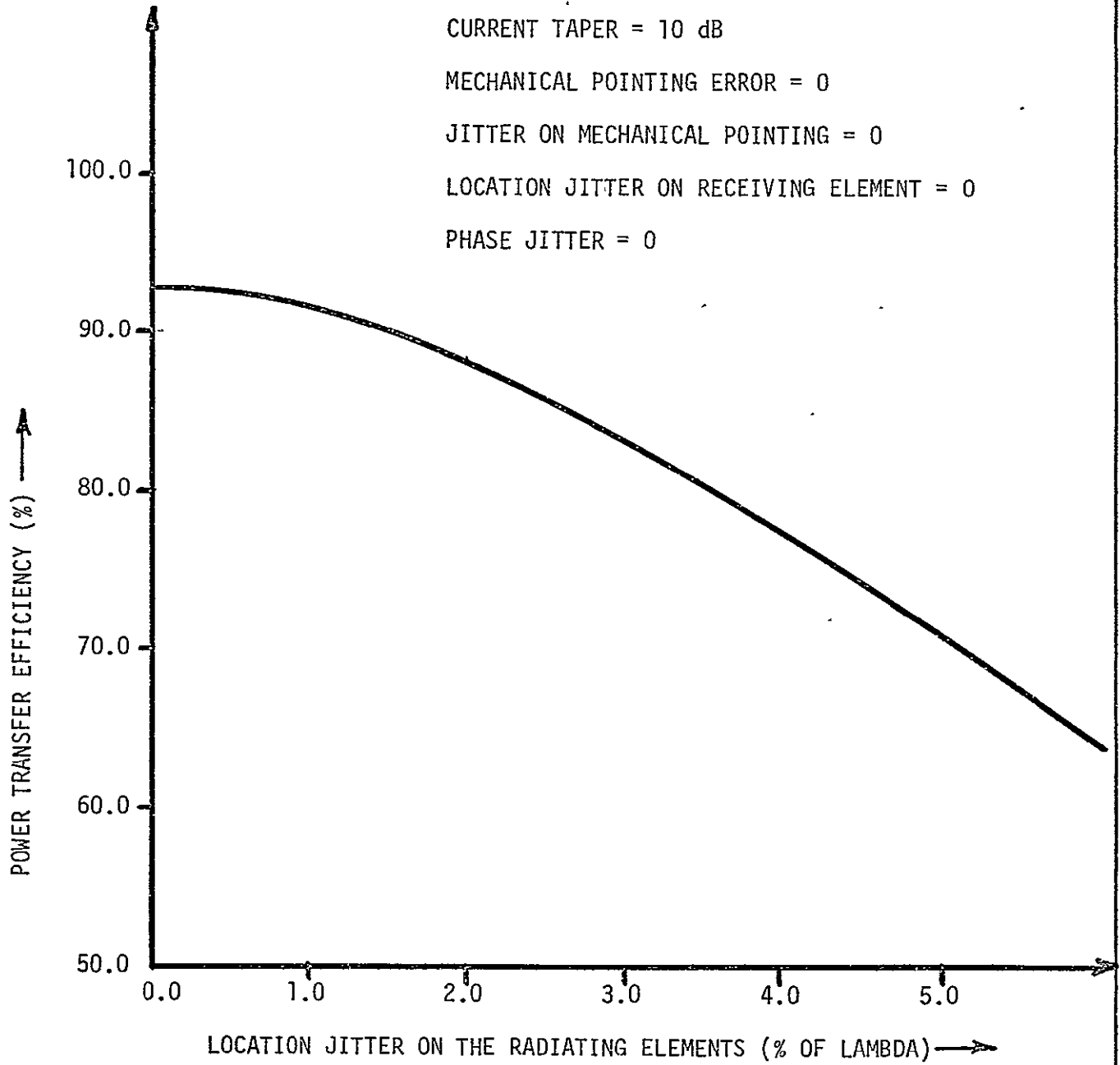


Figure 3.6. Effect of Location Jitter on SPS Power Transfer Efficiency.

80 0086

CURRENT TAPER = 10 dB

MECHANICAL POINTING ERROR = 0

JITTER ON MECHANICAL POINTING = 0

LOCATION JITTER ON RADIATING ELEMENTS = 0

PHASE JITTER = 0

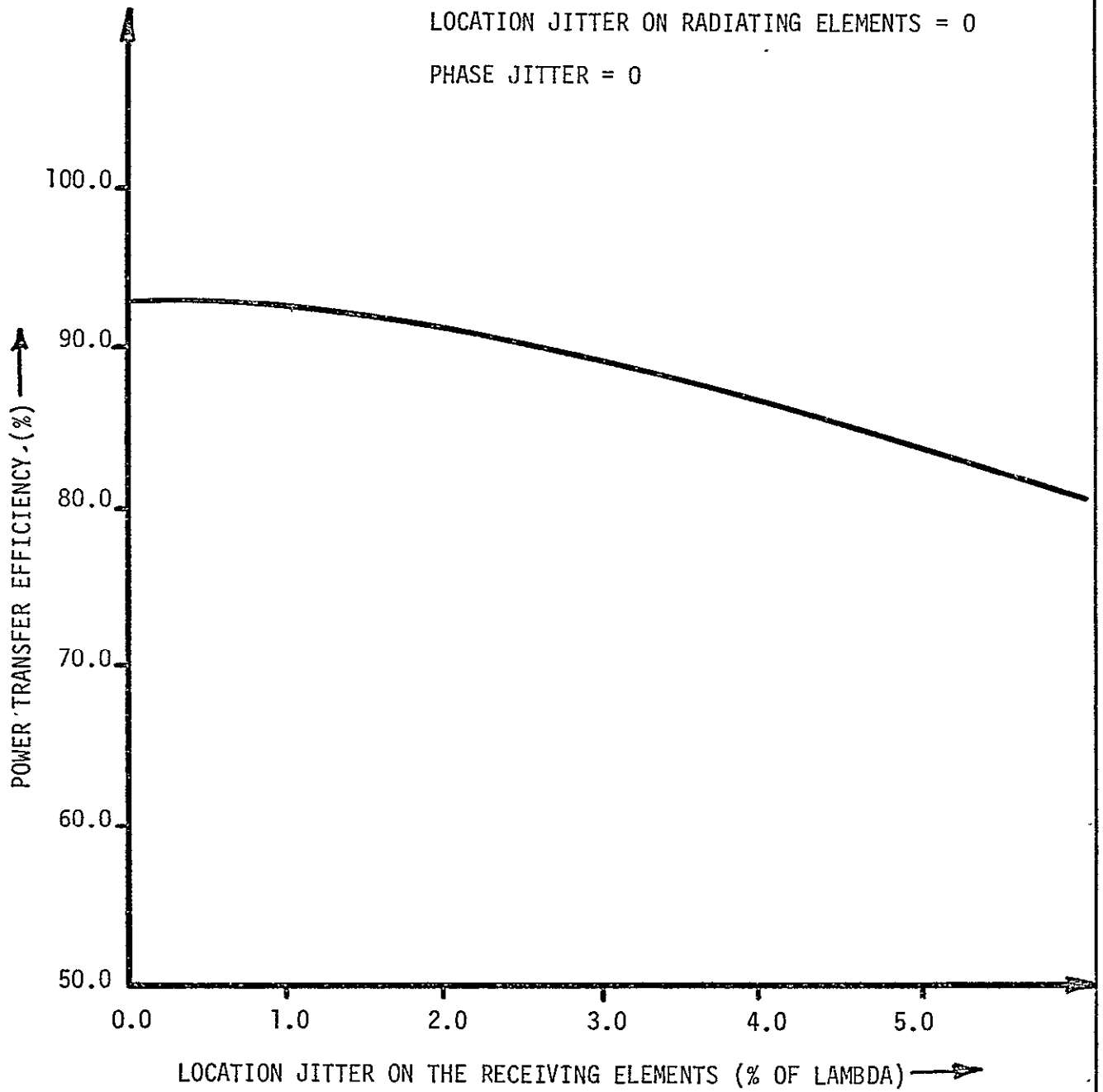


Figure 3.7. Effect of Location Jitter on SPS Power Transfer Efficiency.

80 0087

4.0 EFFECTS OF ANTENNA SYSTEM IMPERFECTIONS ON THE SPACETENNA POWER PATTERN

One of the current capabilities of SOLARSIM is to compute and display the received power pattern. The set of patterns shown in Figs. 4.1 to 4.5 represents its use to investigate the effect of phase error on the received power pattern for the 4-level distribution tree baseline. Fig. 4.1 is a typical power pattern is normalized so that it is unity if all phase error are negligible. This corresponds to a maximum microwave power density of 23 mW/cm^2 at the center of the rectenna. The power pattern is shown as a function of θ which is the angle from the boresight of the spacetenna.- At any point on the rectenna, its distance d from the center is approximately given by $d = R\theta$ where R is the distance of the spacetenna from the rectenna ($3.7 \times 10^5 \text{ Km}$). The edge of the rectenna is approximately equivalent to half a minutes of arc, which is depicted in the figure. Both the power patterns for the 0 dB taper (dashed line) and 10 dB taper (solid line) are shown in Fig. 4.1. We can observe that the power taper serves to bring down the sidelobes while broadening the main beam. For the baseline system (10 dB taper), the power density is down to -13.3 dB at the rectenna edge. This corresponds to a power density of 1.08 mW/cm^2 . The series of figures show that as the phase jitter per level increases, the boresight power density decreases and the sidelobe levels become closer together. Finally, for an rms phase error of 180° per level, i.e., initially no phase control, the spacetenna appears to be an isotropic radiating element (see Fig. 4.5). Under this condition, the power density is approximately $3 \times 10^{-5} \text{ mW/cm}^2$. This level is far below either the U.S. radiation limit (10 mW/cm^2) or the USSR guideline (10^{-2} mW/cm^2) and hence does not appear to pose any biological hazard.

4 LEVEL DISTRIBUTION TREE

SIGMA PER LEVEL = 5°

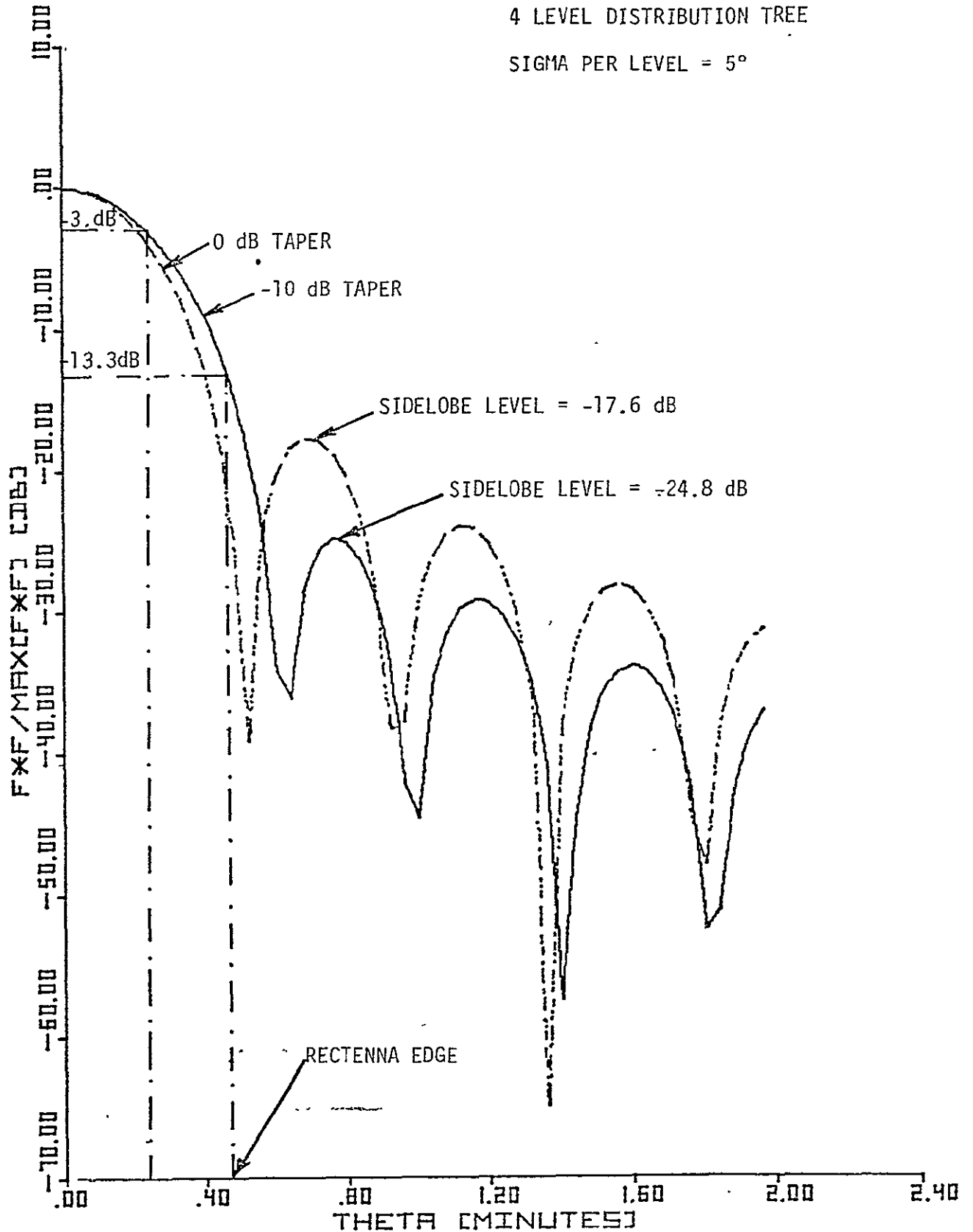


Figure 4.1. Power Pattern for 5° rms Phase Error.

4 LEVEL DISTRIBUTION TREE

SIGMA PER LEVEL = 30°

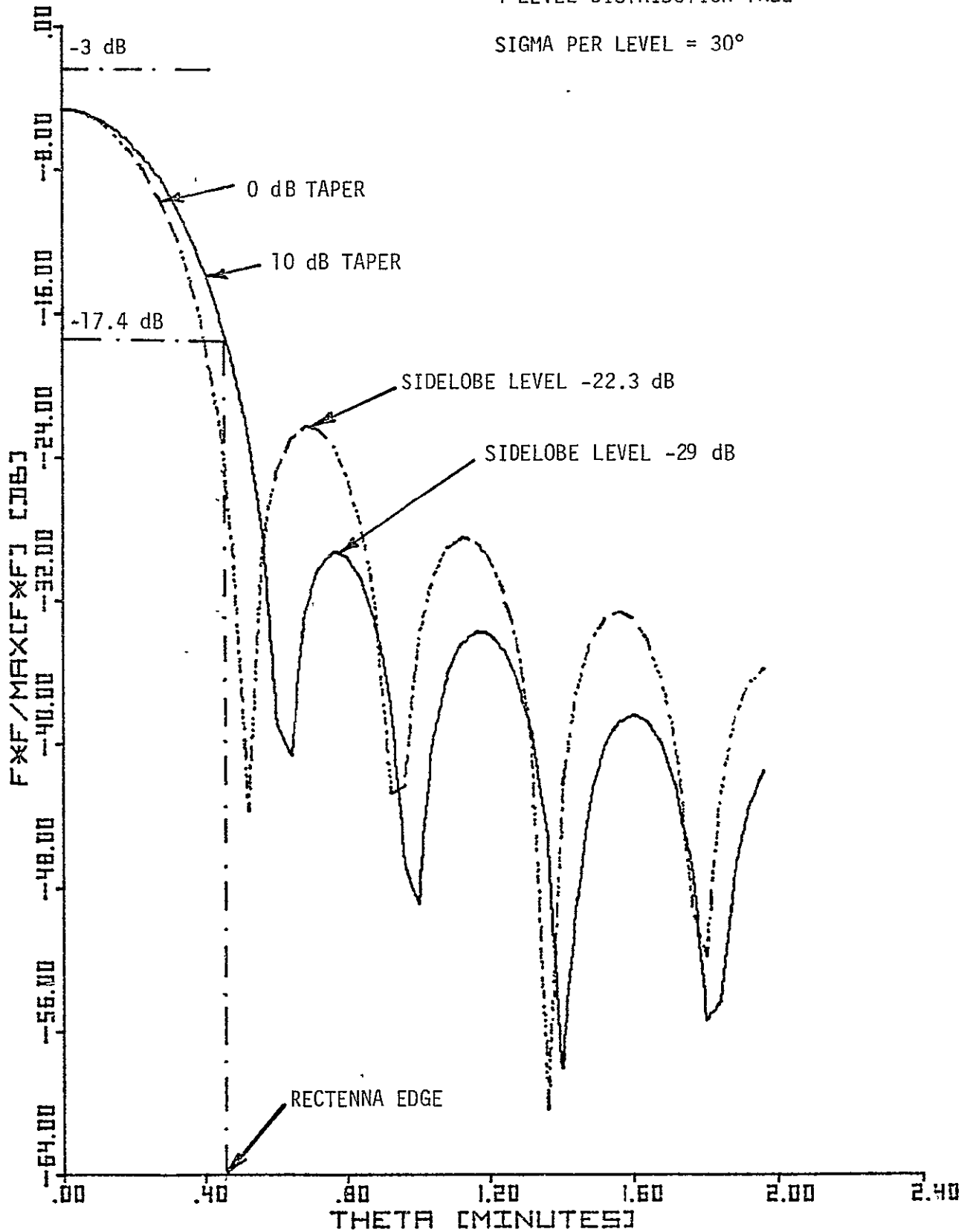


Figure 4.2. Power Pattern for 30° rms Phase Error.

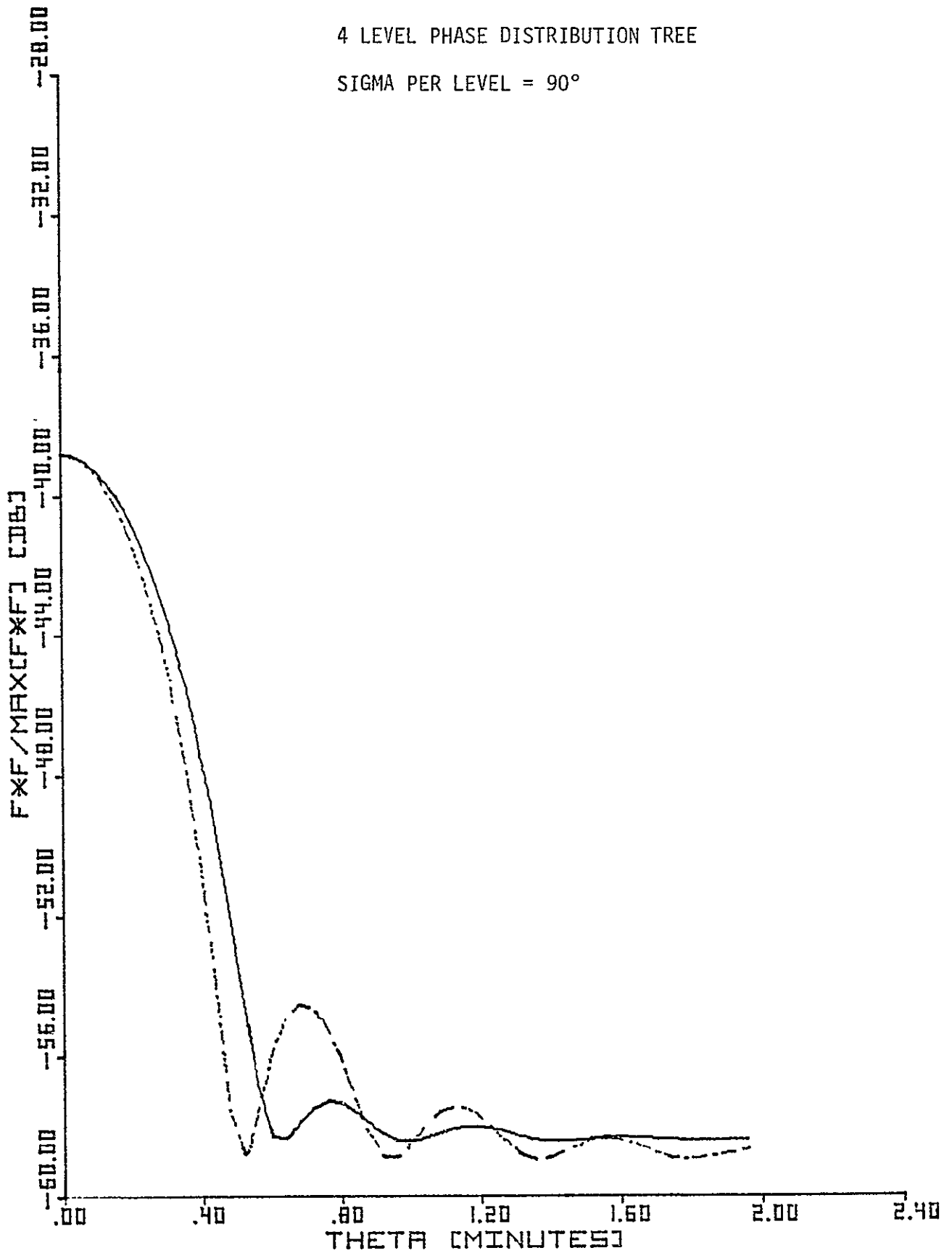


Figure 4.3. Power Pattern for 90° rms Phase Error.

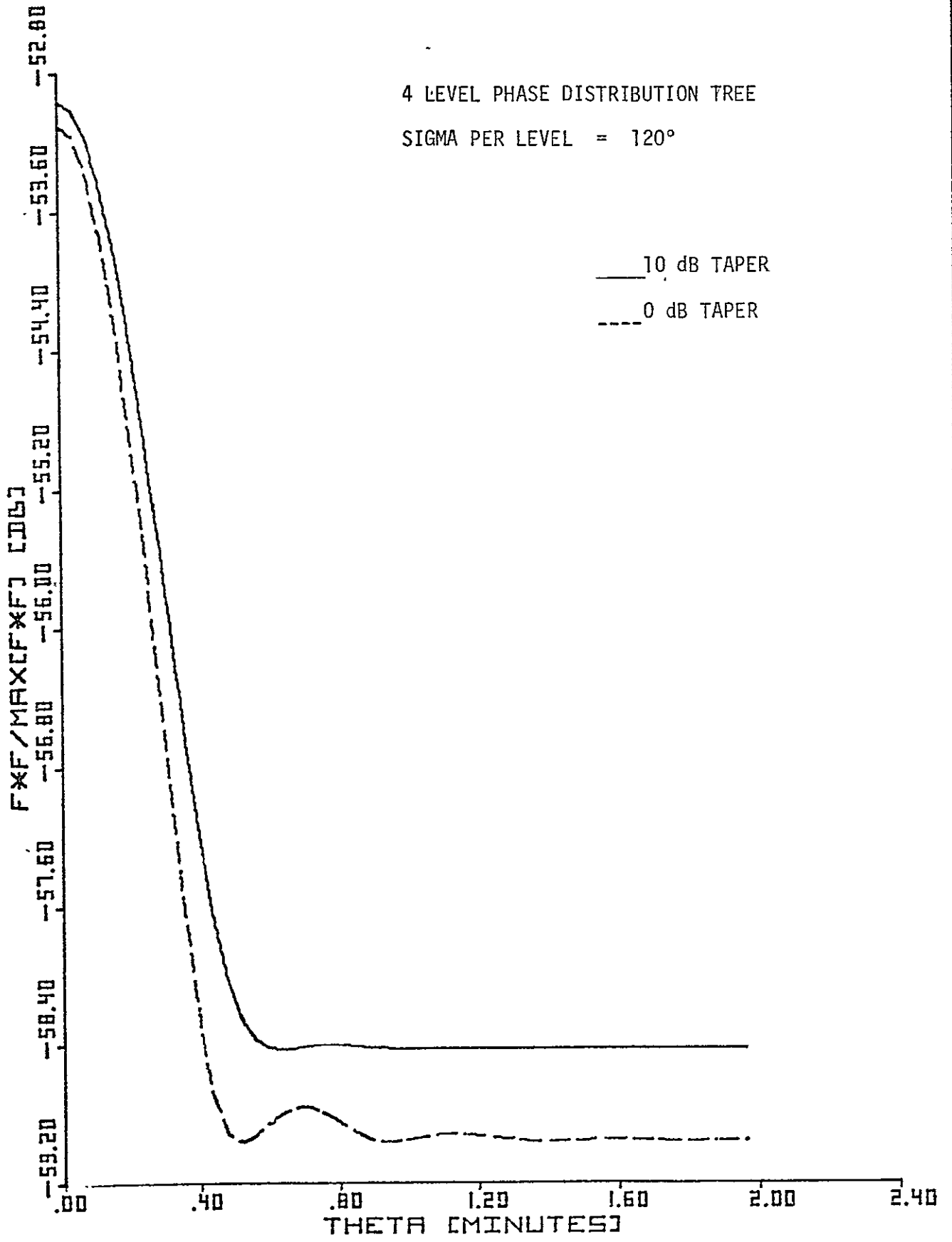


Figure 4.4. Power Pattern for 120° rms Phase Error.

80 0069

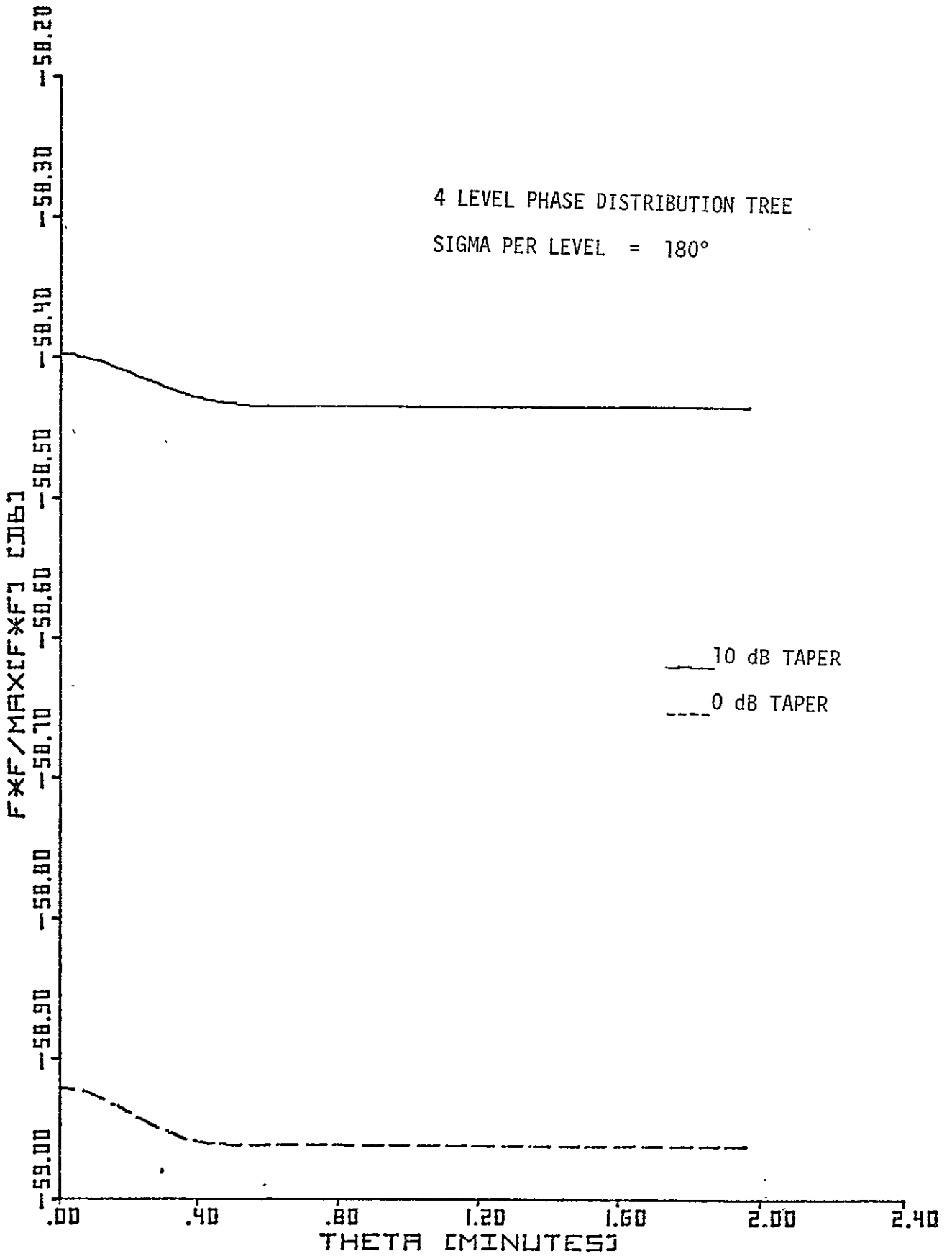


Figure 4.5. Power Pattern for 180° rms Power Error.

80 0070

4.1 Effects of Antenna System Imperfections on the Power Density at the Rectenna

With no system imperfections the power density at the center of rectenna is about 23 mW/cm^2 and the edge of the rectenna it becomes about 1 mW/cm^2 . Even though the SOLARSIM is capable of generating the power density at any point on the rectenna, we will look at the changes of the power density as a function of imperfections at the center of the rectenna only. Effects of the electrical and mechanical imperfections are considered separately.

Fig. 4.6 shows the effect of electrical system imperfections on the power density at the center of the rectenna. For this particular run of the SOLARSIM the mechanical system was assumed to be perfect. On the x axis the label is rms phase error, which is, in effect the phase error added (in the rms sense) by various sources of the electrical system (these sources are listed before). As can be witnessed from the Fig. 4.6, at 10^0 rms phase error. The power density at the center of the rectenna falls to 22.4 mW/cm^2 from 23.1 mW/cm^2 for a perfect system. This is about 3% drop of power density. Thus we can say that in the region of interest ($0-15^0$ rms phase error) the power density is relatively less sensitive to the phase error. Fig. 4.7 is the same as the above figure except that the rms phase error is allowed to get large. Even at 50^0 rms phase error, the power density at the center of rectenna is 10 mW/cm^2 .

The next three figures describe the effect of mechanical system imperfections on the power density at the center of rectenna while the electrical system is assumed to be perfect. The mechanical imperfections considered are: (1) location jitters (LJ) on radiating and pilot receiving elements, (2) the mechanical pointing error (MPE) of

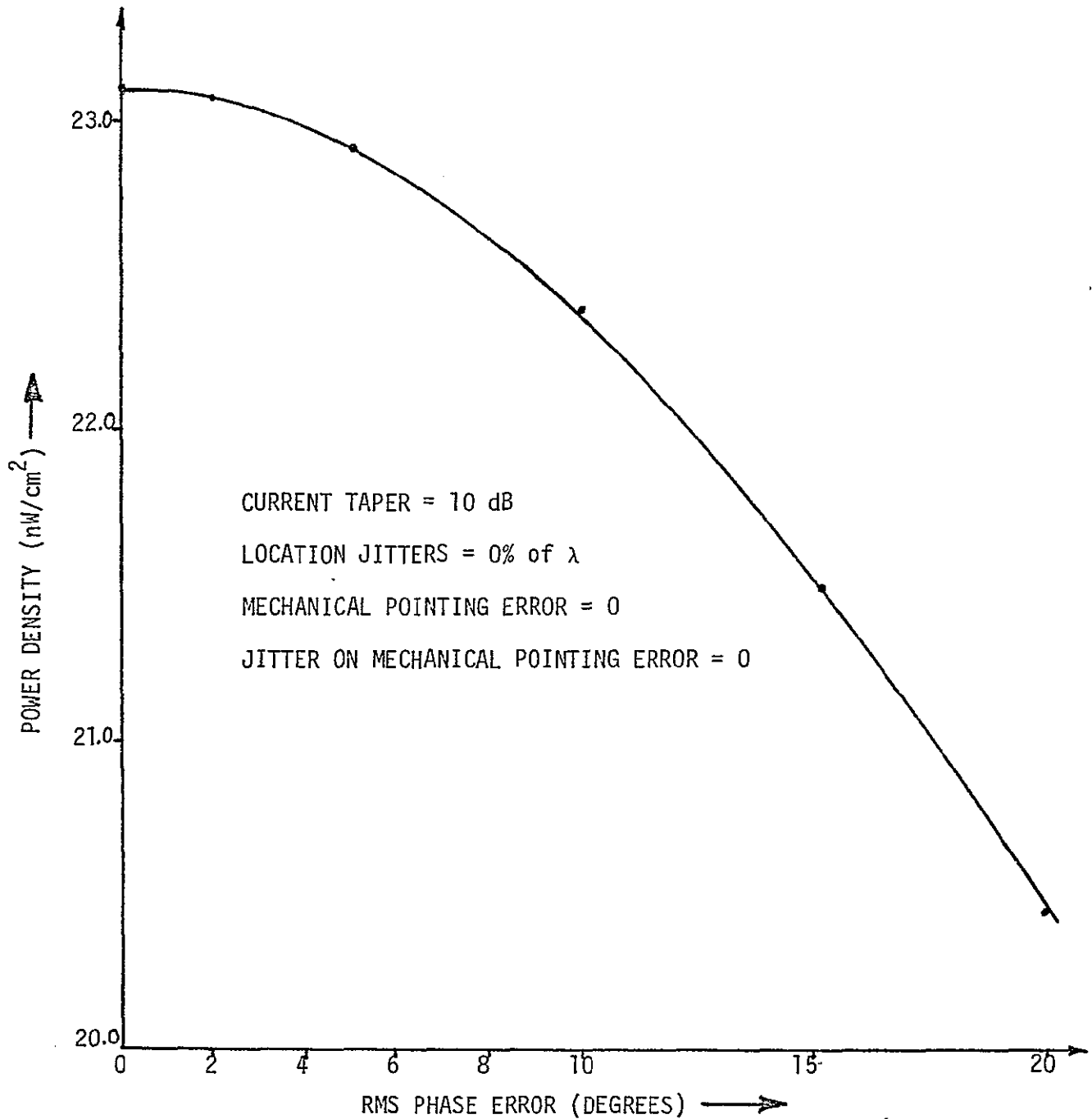


Figure 4.6. Effect of Phase Error on Received Power Density Level.

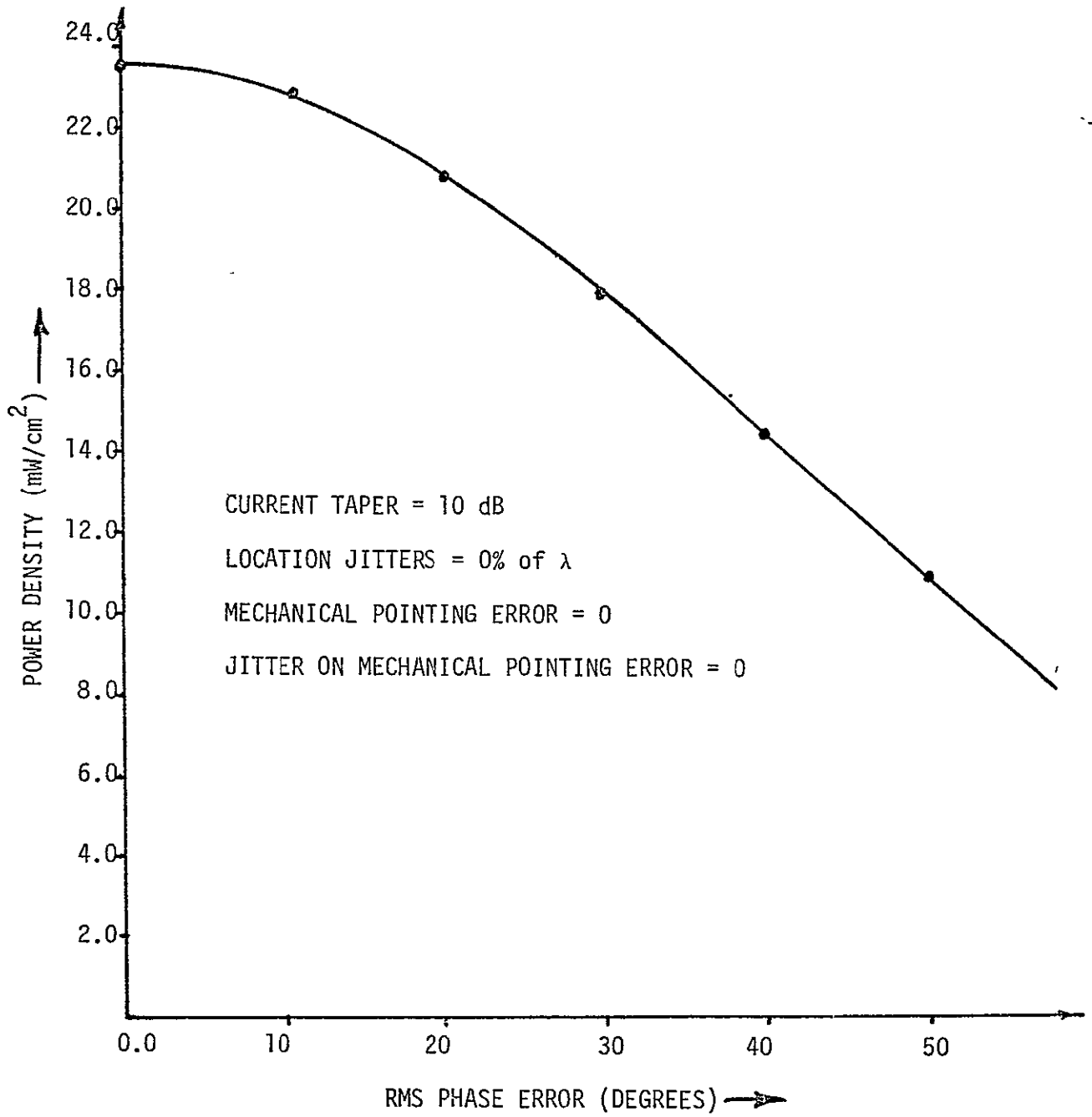


Figure 4.7. Effect of Phase Error on Received Power Density Level.

80 0072

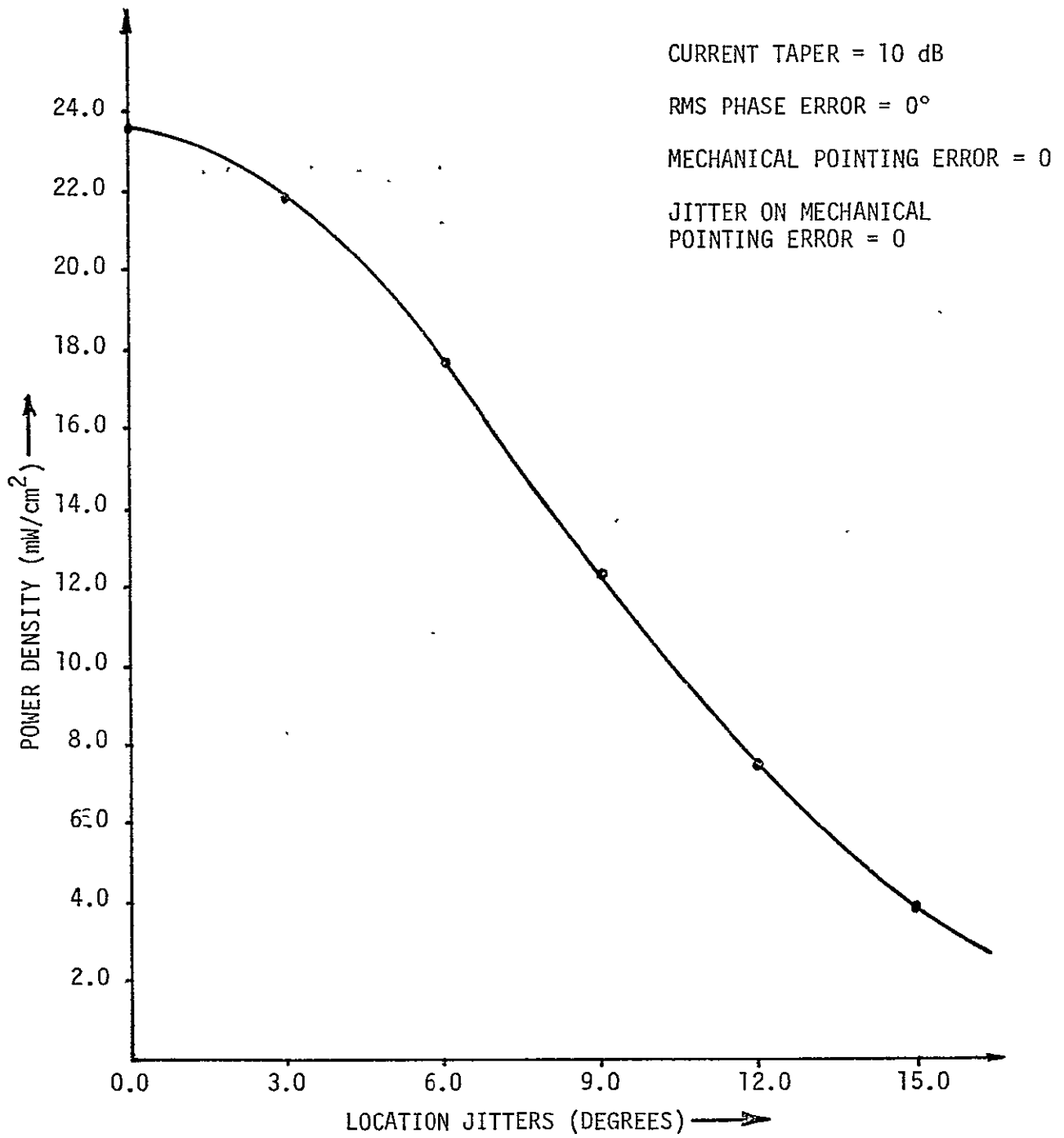


Figure 4.8. Effect of Location Jitters on Received Power Density Level.

80 0073

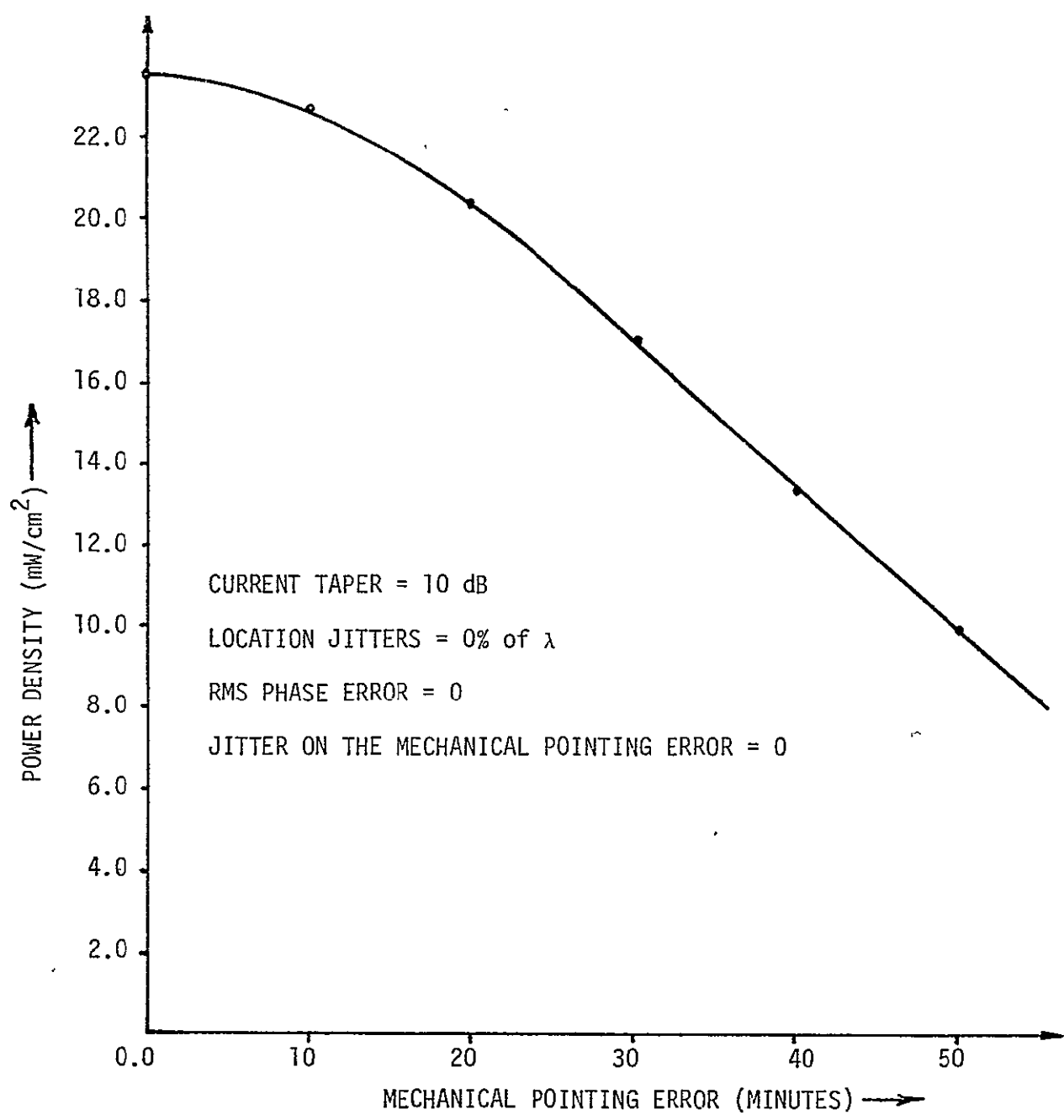


Figure 4.9. Effect of Mechanical Pointing Error on Received Power Density Level.

80 0074

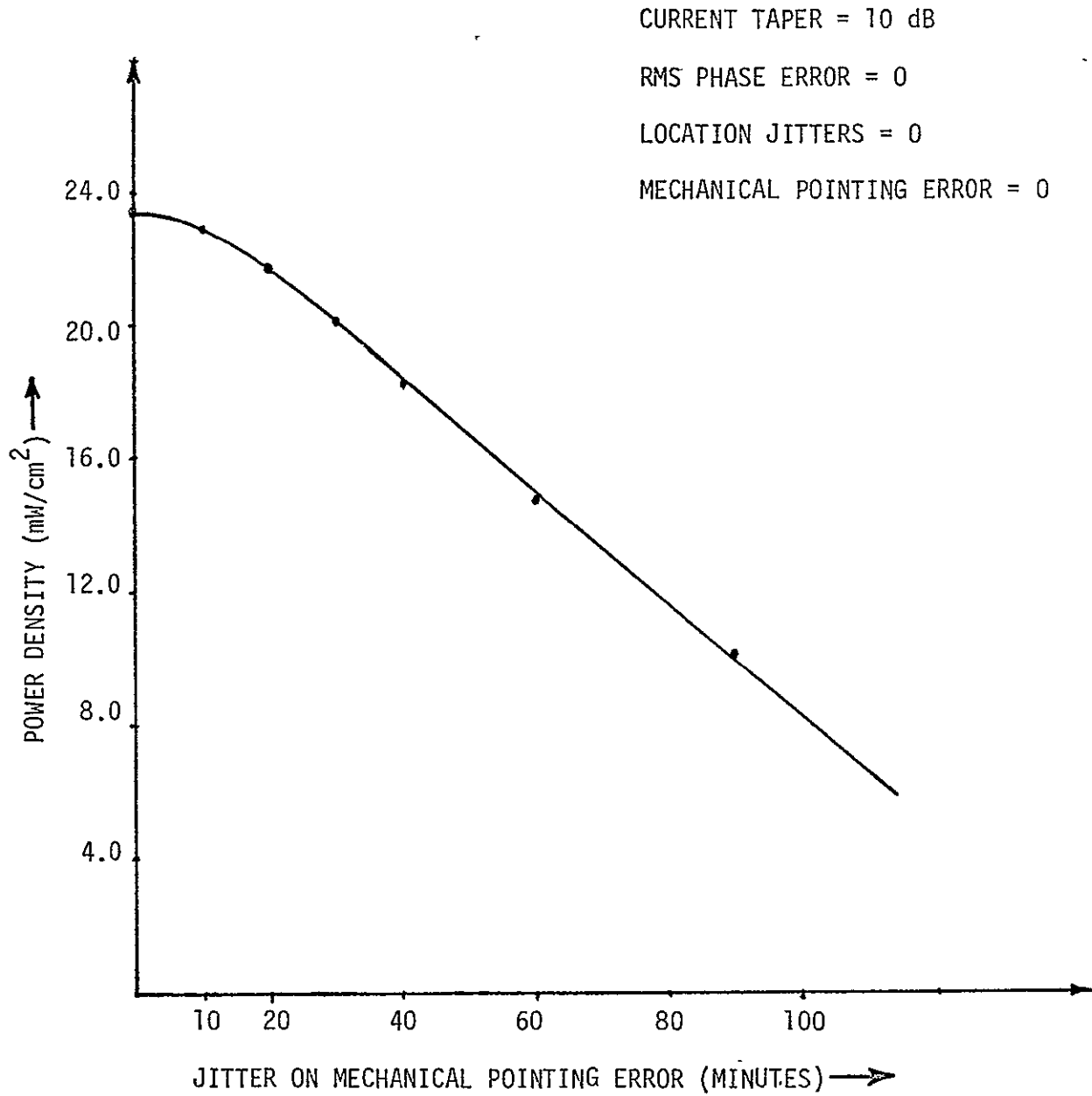


Figure 4.10. Effect of Mechanical Pointing Jitter on Received Power Density Level.

80 0088

the subarrays and (3) the jitters on mechanical pointing error. In each figure the electrical system is perfect and only one mechanical imperfection varies while the remaining mechanical imperfections are held to zero. It can be seen that in the region of the interest (i.e., LJ on radiating and transmitting elements $\epsilon (0, 2\% \lambda)$, MPE $\epsilon (0, 10')$ and jitter on MPE $\epsilon (0, 2')$) the power density at the center of the rectenna does not fall below 22 mW/cm^2 . For a more realistic case when total rms phase error = 10° , LJ on receiving as well as transmitting elements = $2\% \lambda$, MPE = $10'$ and jitter on MPE = $2'$ the power density at the center of rectenna falls to 20.93 mW/cm^2 and the density at the edge of the rectenna equals 1.1 mW/cm^2 .

5.0 EFFECT OF SYSTEM IMPERFECTIONS ON THE MAIN BEAM GAIN LOSS

As we saw above, there are two different types of imperfections, i.e., electrical and mechanical system imperfections. Each kind has its own effect on the main beam gain. We will discuss the effects of electrical and mechanical imperfections on the main beam gain separately.

5.1 Effect of electrical System Imperfections on the Main Beam Gain Loss

The main beam gain reduction is a function of the magnitude of and the level where the phase errors are introduced by the phasing tree. It is interesting to see the extent to which the phase errors introduced at each level individually contributes to reduce this gain. In Fig. 5.1 we show the effect of the phase errors introduced at a particular level in the phase distribution tree, while the phase error at the other levels are neglected. A phase jitter of 5° is shown for a four level tree. The normal main beam gain loss of gain in dB is plotted in Fig 5.1.

The quantity G_0 is obtained when all the phase errors introduced in the phasing tree are set to zero. From Fig. 5.1 we see that as far as

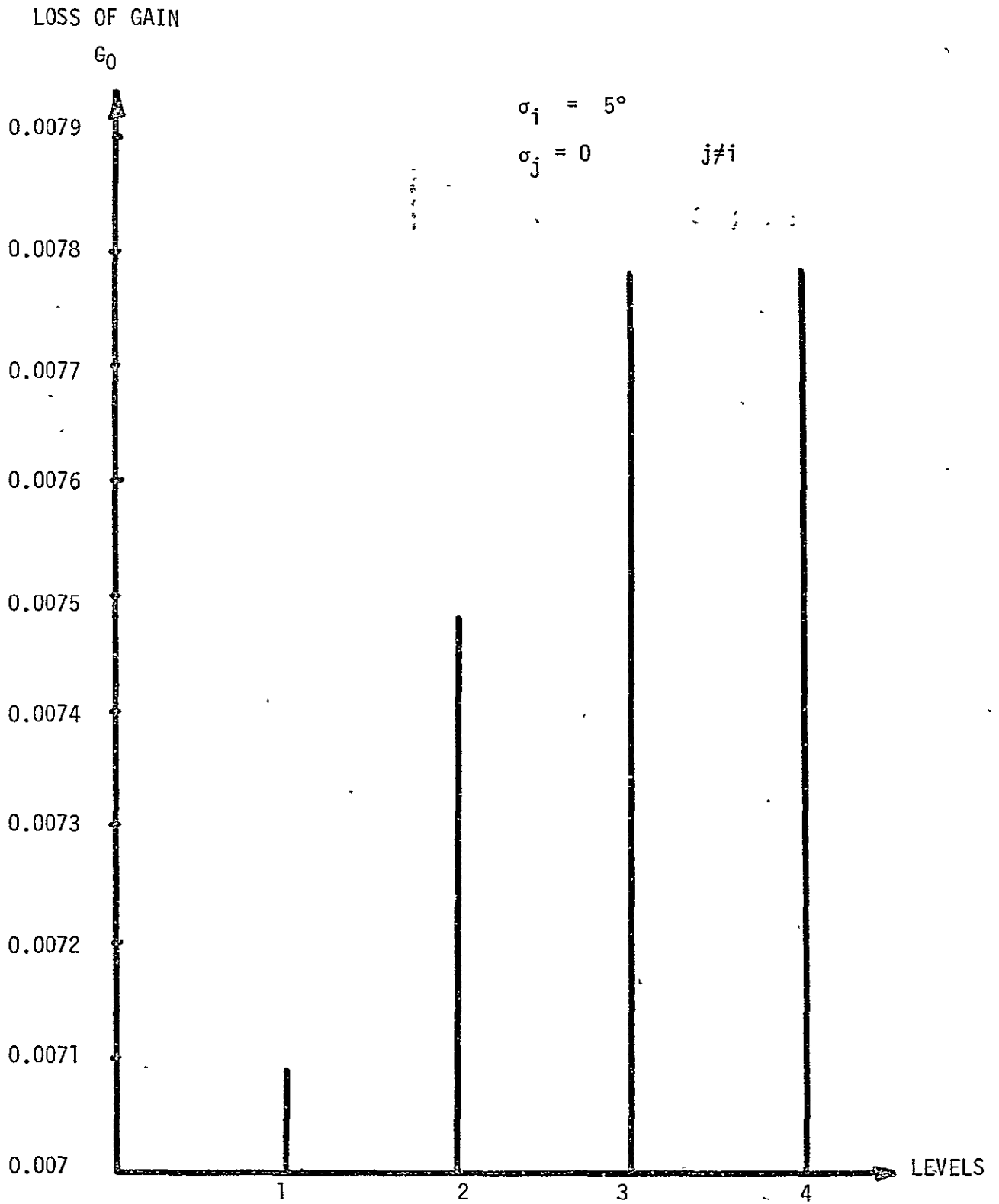


Figure 5.1. Effect of Phase Jitter Introduced in Different Levels of the 4-Level Phase Reference Tree.

80 0075

the gain reducing is concerned, phase errors introduced in the last level (4th level) results in the worst performance. Intuitively, phase errors introduced at the beginning levels of the tree cause the total phase error build up at the radiating elements to be correlated. As a result, individual patterns all add up in the same general direction. On the contrary, when phase errors are introduced in the last level, radiating elements have uncorrelated phase errors which results in reduced main beam gain. In any case, the differences are small.

We have seen qualitatively how the efficiency of the microwave transmission system is reduced if the phase error build up is not kept under control. Fig. 5.2 investigates this effect by plotting the boresight gain reduction vs the total rms phase error build up through the phasing tree. As we have seen earlier, the shape of the power pattern is relatively insensitive to the phase error, at least to the first few lobes shown provided the rms phase error is not excessive (e.g. $\leq 30^\circ$). In that case, the main beam reduction is proportional to the power received by the rectenna. In Fig. 5.3 and in what follows, total rms phase error is defined to be the total phase error build up through the phase distribution tree, assuming each level in the tree adds in the same amount of phase error. The phase error processes introduced at different nodes on the same level are assumed to be independent of one another. For an efficiency of 96%, Fig. 5.3 indicates that one can only tolerate about 11.8° of total rms phase error. The allowable phase error build up in the tree structure for a fixed efficiency is tabulated in Fig. 5.3. For the 96% efficiency, the total (RF) phase error build-up of 11.8° reflects into an IF phase error build-up of 2.4° for the 490 MHz IF baseline. For a four level tree

MAIN BEAM GAIN
REDUCTION (dB) ; G/G_0

LinCom

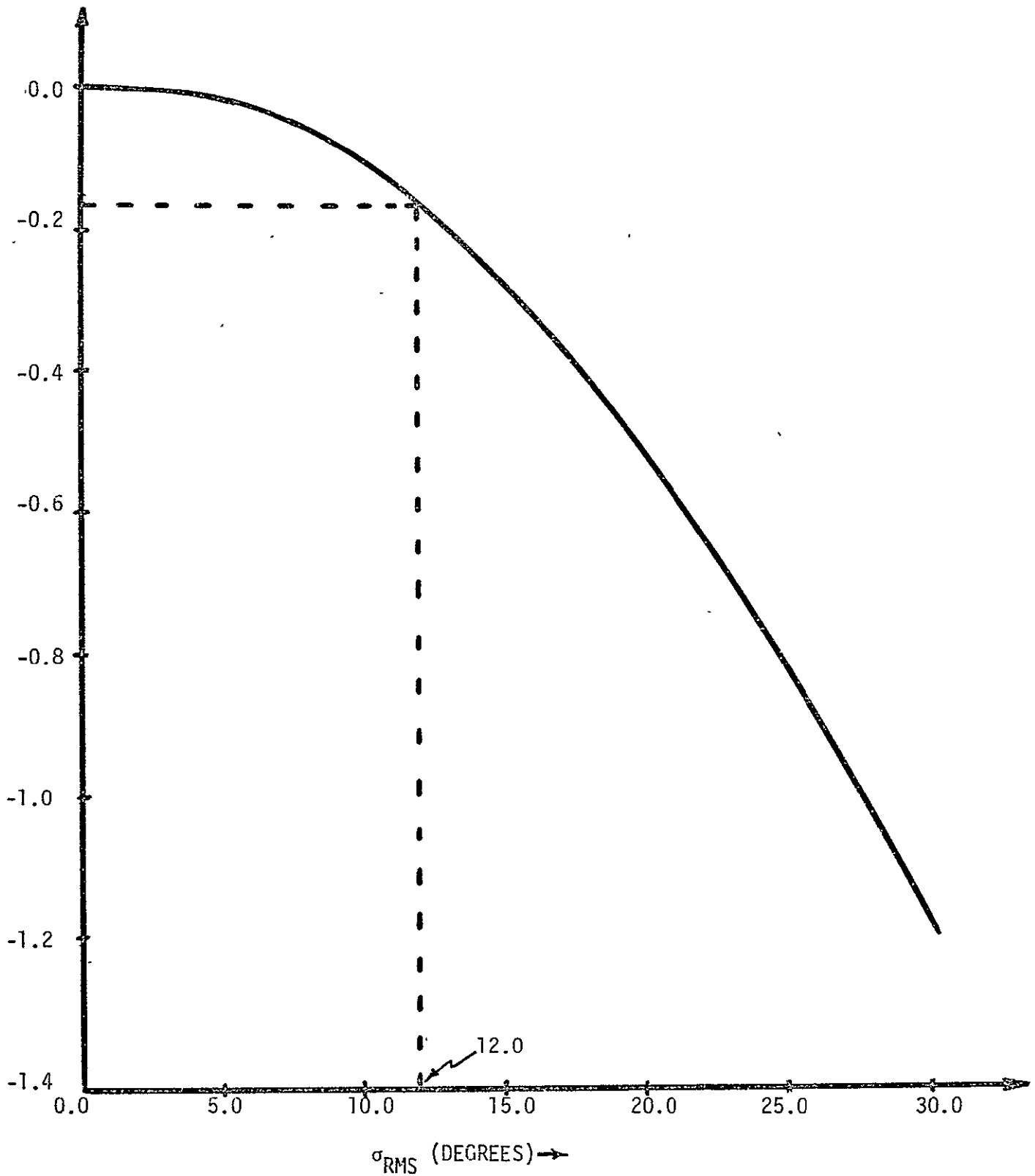


Figure 5.2. Main Beam Gain Reduction Due to Phase Error Build Up in Tree of Phase Control System.

ED 0076

G/G ₀ EFFICIENCY (PERCENT)	PHASE ERROR BUILD UP (DEGREES)			
	TOTAL RF P.E. BUILD UP°	TOTAL IF P.E. BUILD UP°	RF P.E. BUILD UP PER LEVEL	
			L=9	L=4
96.0	11.8	2.4	3.93	5.9
90.0	18.8	3.8	6.5	9.7
85.0	23.0	4.6	7.7	11.5
80.0	27.0	5.4	9.0	13.5
75.0	30.5	6.1	10.17	15.25

Figure 5.3. Efficiency Performance of Baseline Phase Distribution System vs Phase Error Build Up.

(baseline system) the maximum error tolerable is 5.9° per level. If a nine level tree is used, we have to tighten the phase error specification to 3.9° per level. In his respect, the 4 level tree system seems to be superior. However, since different amounts of hardware and layout is required for different structures, the above remark is not conclusive.

As we have seen earlier, the phase errors introduced at the last level result in the most severe reduction in the main beam gain. This effect is further investigated in Fig. 5.4 in which the total phase error build up through the phasing tree up to, but excluding the last level, is held fixed at 15° rms, and we vary the phase error introduced at the last level. The resultant gain reducing is identical for the four and the nine level tree. In general, one expects the magnitude of the phase error introduced in the last level to be higher than the earlier levels, since we must now take into account the phase errors introduced by the power transponder, in addition to the phase reference distribution system.

5.2 Effects of Mechanical System Imperfectionss on the Loss of Gain

The mechanical imperfections can be applied to two different entities: the radiating elements and the conjugating elements.

In the absence of tilt effects, the performance of the spacetenna is not sensitive to the conjugation levels. In practice, the presence of tilt effects determines the level required. Fig. 5.5 compared the sensitivity of the gain reduction G/G_0 vs the mechanical pointing error with the location jitters (assumed equal for conjugation points and radiating elements) as a parameter. A typical rms tilt $\sigma_\theta = \sqrt{\sigma_{\theta_x}^2 + \sigma_{\theta_y}^2}$ of 2 mrad is assumed. We can observe that the baseline system degrades

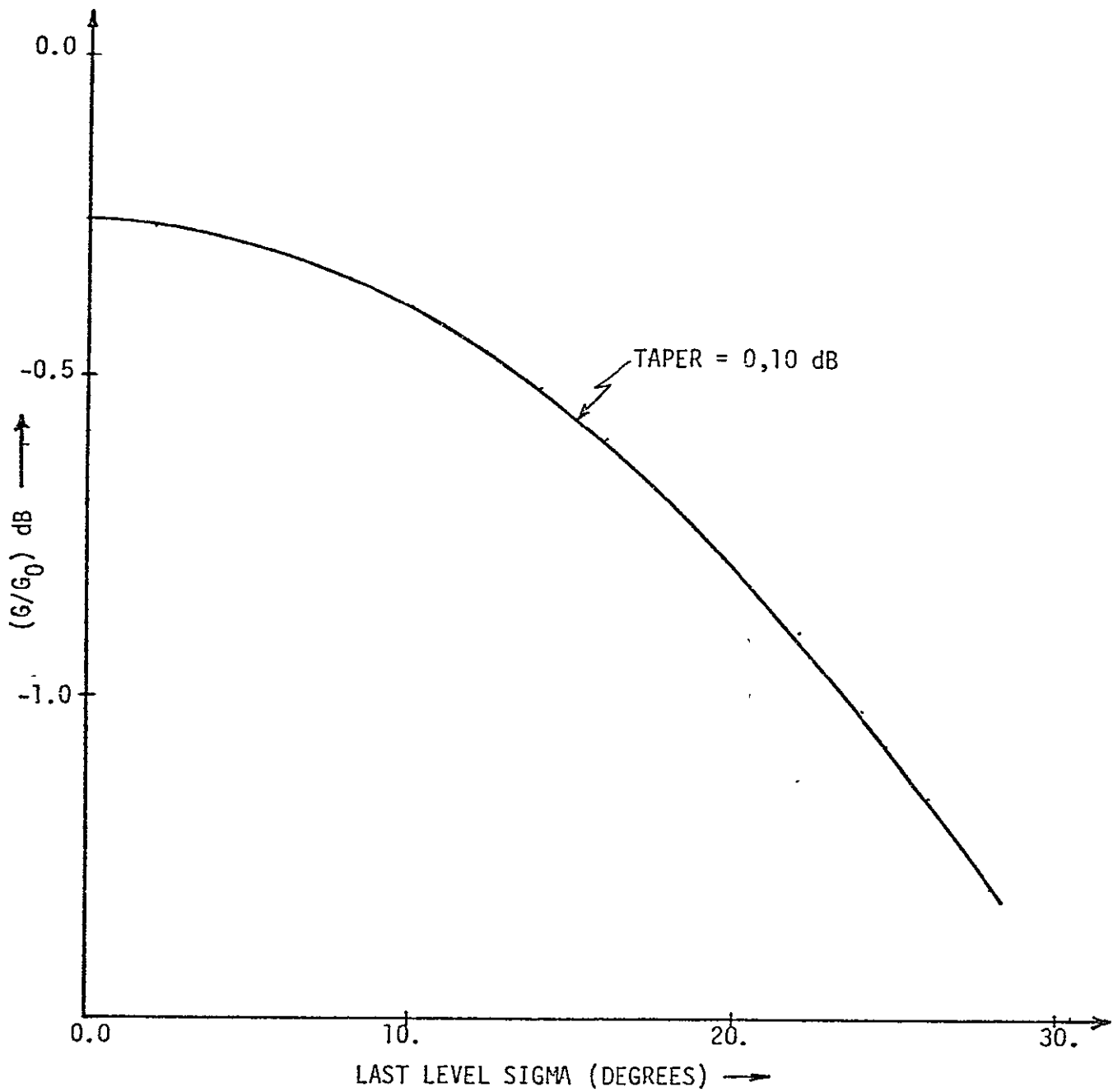


Figure 5.4. Gain Reduction for 4 and 9 Level Trees with the Last Level Sigma Changing.

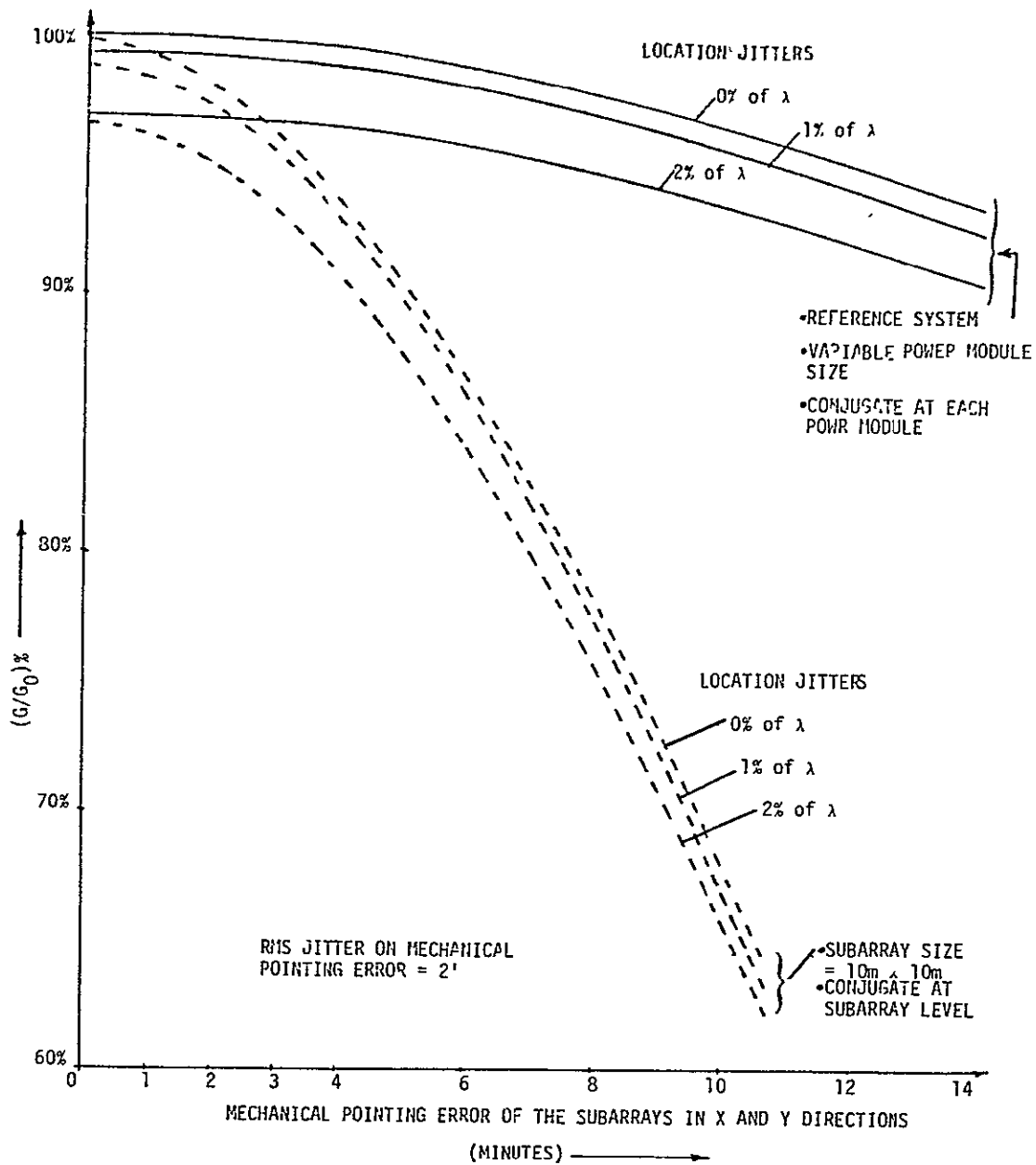


Figure .5.5. Sensitivity to Tilt Effects as a Function of Phase Conjugation Level.

80 0079

more gracefully than the fixed subarray (Boeing) scheme.

6.0 EFFECTS OF SYSTEM IMPERFECTIONS ON THE POINTING ERROR

When there are no imperfections (electrical or mechanical) present in the spacetenna systems, the focusing of the power beam is perfect, i.e., the power beam is focused at the center of the rectenna with all the individual radiating elements phased properly so as to maximize the boresight gain. When the random errors (system imperfections) are introduced, the spacetenna power pattern peaks at some direction other than the boresight. The variance of this direction is the spacetenna pointing error. Currently SOLARSIM has the capacity to evaluate the pointing error due to the imperfections due to the electrical system only.

Depending on the level where phase errors are introduced, the resulting pointing error is different. From Fig. 6.1 we can see that the phase error introduced at the first level causes the largest rms pointing error while the phase error from the last level (level four) has the least impact. The same trend is observed from the 8- and 9-level phase distribution tree which is depicted in Fig. 6.2. In essence, if independent phase errors are introduced at the last level, the resultant phase error variance on the beam is reduced roughly by the number of radiating elements (101,552). This follows from the law of large numbers. However, if the phase errors are introduced at the first level, the resultant phase error variance on the beam is reduced by the number of nodes in the first level. For the baseline (4-level tree), that number is 25. The square root of the ratio $101,552/25$ is roughly 18 dB, which can be observed in Fig. 6.1.

The sensitivity of the rms pointing error to the total phase error

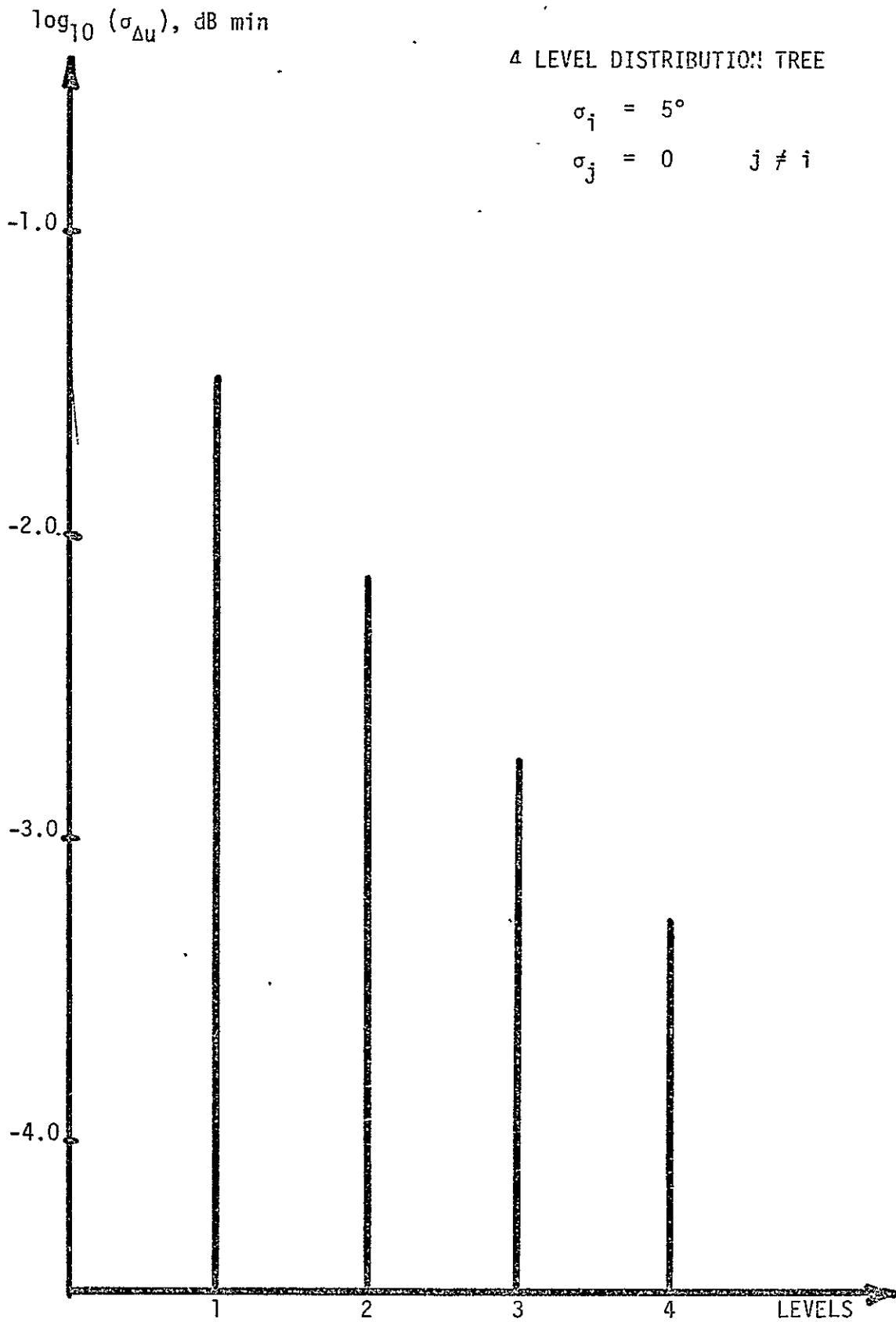


Figure 6.1 RMS Pointing Error as a Function of the Level When Phase Errors are Introduced for a Four-Level Tree.

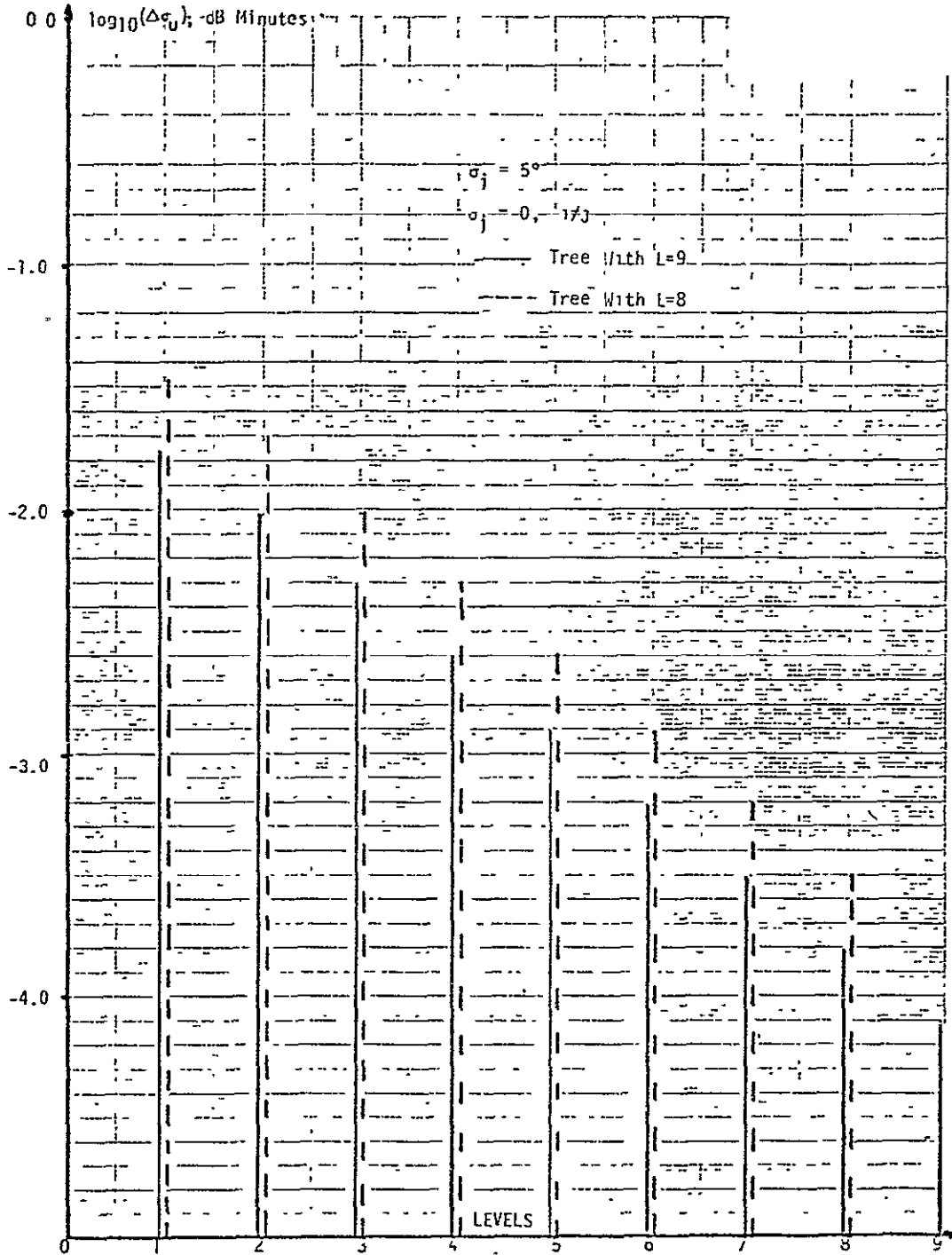


Figure 6.2. RMS Pointing Error as a Function of the Level where Phase Errors are Introduced.

ORIGINAL PAGE IS
OF POOR QUALITY

80 0081

build up is investigated in Fig. 6.3. As to be expected, the pointing error is directly proportional to the phase error. It is of interest to relate the rms pointing error to the probability that the beam misses the rectenna center by a given amount. This is rather straightforward if we assume that the pointing error is approximately Gaussianly distributed. For a typical total rms phase error of 15° , we can see from Fig. 6.3 that the rms pointing error is 0.019 mrad. This translates into a probability of 0.99 that the main beam will be restricted to 0.03 mrad off boresight. In terms of distances, this means that the probability that the main beam misses the rectenna center by 300 meters is less than 10^{-2} .

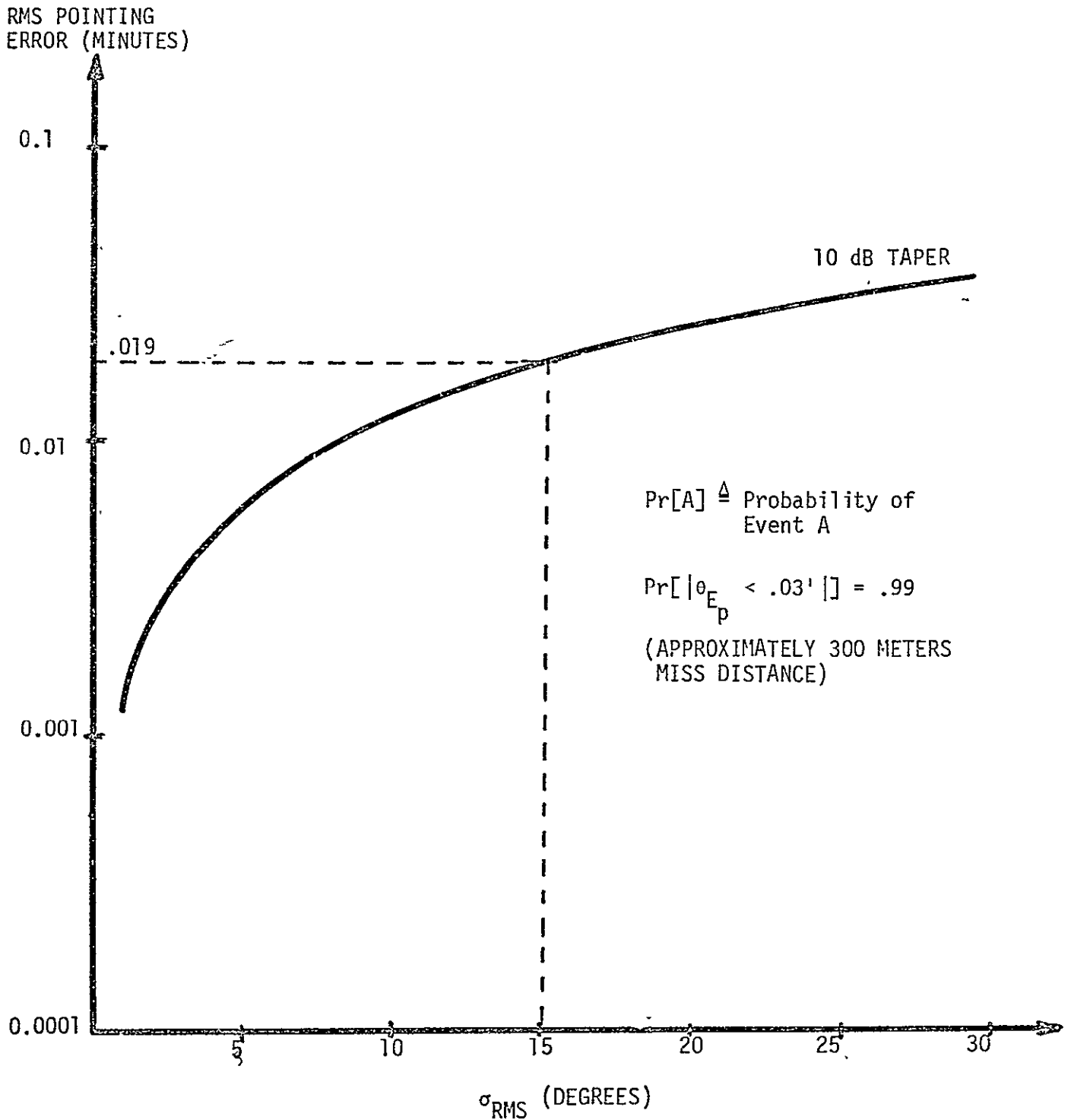


Figure 6.3. RMS Pointing Error Due to the Phase Error Build Up in Tree of the Phase Control System.

REFERENCES

1. Lindsey, W. C., "A Solar Power Satellite Transmission System Incorporating Automatic Beam Forming, Steering and Phase Control," Prepared for NASA/JSC, TR-7806-0977, June, 1978, LinCom Corporation, Pasadena, CA.
2. Lindsey, W. C., and Kantak, A. V., "Automatic Phase Control in Solar Power Satellite Systems," Prepared for NASA/JSC TR-7809-0977, September 1977, LinCom Corporation, Pasadena, CA.
3. Lindsey, W. C., and Kantak, A. V., "SPS Phase Control System Performance via Analytical Simulation," Prepared for NASA/JSC, TR7903-0977, February, 1979, LinCom Corporation, Pasadena, CA.

APPENDIX. PROGRAM STATUS

I. SOLARSIM SPS System Definition and Computational Considerations

1. Spacetenna: Spacetenna is a stepped approximation of a circle of 1 Km diameter having an area of $0.76 \times 10^6 \text{ mt}^2$. This area is subdivided into subarrays. The total number of power amplifiers (klystrons) in the spacetenna is $101,552 = N$. The operation of spacetenna is retrodirective, i.e. the uplink pilot from the earth based rectenna delivers the phase to be conjugated at the spacetenna conjugators and then the conjugated phase is used on the outgoing power beam for retrodirection. The convention followed is: (θ_r, ϕ_r) is the direction of the pilot beam as seen from the spacetenna center.

2. Current Taper: For the control of side lobes of the spacetenna, an excitation current taper of 10 dB (center to edge taper) is suggested for the control of side lobes. This taper is implemented by discretizing the taper into ten levels and putting different number of amplifiers per unit area from level to level. It should be noted that the rating of the power amplifiers is the same all over the antenna. The ten levels when imposed on the circular spacetenna become ten circles having different number of power amplifiers per unit area from circle to circle.

The following convention is followed:

NA(I) Total number of amplifiers in the i^{th} density circle
 $I = 1, 2, \dots, 10$

R(I) The radius of the i^{th} power density circle, $I = 1, 2, \dots, 10$.

Figure 1 shows the figure of the spacetenna with the ten power density circles, their radii and the number of power amplifiers in each circle. Even though the current rating of the power amplifiers is the same, the current density is different for different power rings. These current

densities are designated $CURNT(I)$, $I = 1, \dots, 10$, and the amplitude jitters associated with the currents in terms of the percentage of the amplitudes. These are designated as $SIGMAI(I)$, $I = 1, \dots, 10$.

3. Subarrays: The baseline system assumes only one power amplifier per subarray. Since there are different numbers of amplifiers present per unit area in different power density rings, the size of subarray is different from ring to ring. The subarrays are assumed to be square and have the power amplifier and the phase conjugation circuitry at its geometric center. The actual radiating elements are the slots in the waveguides. Figure 1 shows the size and number of subarrays in each power ring. One alternate way is to have a constant sized square subarray throughout the spacetenna. Such an arrangement will have a different number of power amplifier per subarray from ring to ring. This arrangement is also shown in Figure 1. The following convention is followed:

$N(I)$ The number of radiating slots in i^{th} power ring
 $I = 1, \dots, 10$

$M(I)$ The number of radiating slots per subarray in i^{th}
 power ring, $I = 1, \dots, 10$.

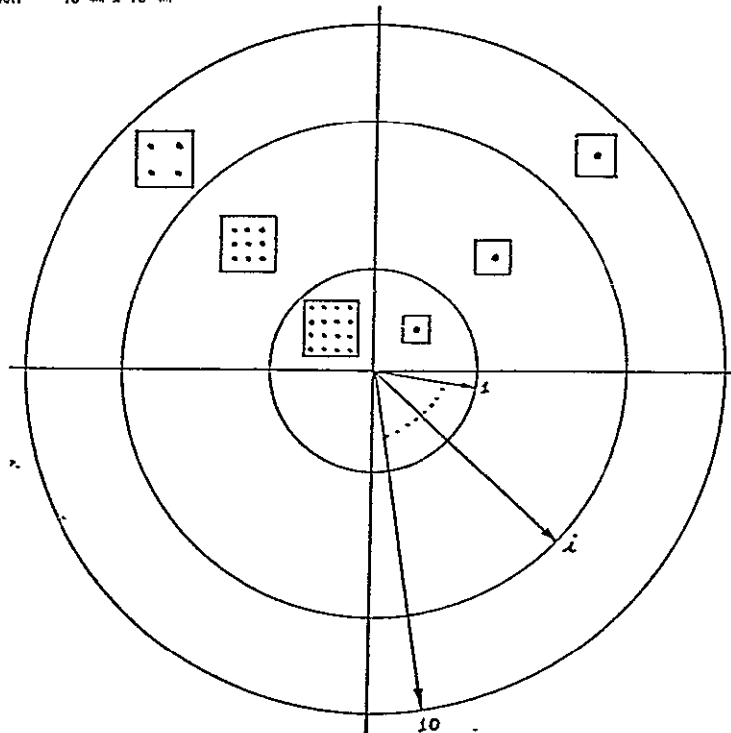
4. Tilts on the Subarrays: There are basically one type of tilt and two types of tilt jitters associated with the subarrays. Mechanical tilting of the subarrays with respect to x and y directions. This tilting has a mean value and a jitter associated with it. The mean value of the tilt gives the mechanical tilt of the spacetenna as compared to perfectly pointed spacetenna. There are two components of this tilt and each component has a jitter on it. The jitters one has to

Figure 1.

VARIABLE AND FIXED SIZE SUBARRAY-GEOMETRY

POWER DENSITY STEP	NUMBER OF SUB-ARRAYS	NUMBER OF POWER MODULES PER CONJUGATION PT	TOTAL # OF POWER MODULES PER DENSITY STEP	POWER DENSITY STEP	SIZE OF SUBARRAY	NUMBER OF SUBARRAYS	TOTAL # OF POWER MODULES PER CONJUGATION POINT	# OF POWER MODULES
1	276	36	9936	1	1.73m x 1.73m	9936	1	9936
2	632	30	18960	2	1.89m x 1.89m	10960	1	18960
3	644	24	15456	3	2.12m x 2.12m	15456	1	15456
4	628	20	12560	4	2.32m x 2.32m	12560	1	12560
5	784	16	12544	5	2.6 m x 2.6 m	12544	1	12544
6	900	12	10800	6	3. m x 3 m	10800	1	10800
7	664	9	5976	7	3.46m x 3.46m	5976	1	5976
8	612	8	4896	8	3.67m x 3.67m	4896	1	4896
9	1052	6	6312	9	4.24m x 4.24m	6312	1	6312
10	1028	4	4112	10	5.2 m x 5.2 m	4112	1	4112
TOTAL FOR FULL ARRAY	7220		101552			101552		101552

SIZE OF THE SUBARRAY = 10.4m x 10.4m



worry about are the location jitters of the radiating and conjugating (pilot receiving) elements. These jitters actually have three components: two components in the plane perpendicular to the line joining that particular element and the rectenna center and one component along that line. We will neglect the components in the plane and consider only the jitter component along the line joining the element and the rectenna center as the location jitter of the element. The convention followed is given in the following table.

Mean Mechanical Tilts of the Subarrays	$X_{MEAN}(I), Y_{MEAN}(I)$ $I = 1, 2, \dots, 10$
Jitters on Mechanical Tilts	$SIGMA(I), I = 1, 2, \dots, 10$
Location Jitter on the Pilot Receiving Element	$SIGPSI(I), I = 1, 2, \dots, 10$
Location Jitter on the Radiating Element	$SIGPHI(I), I = 1, 2, \dots, 10$

It should be noted that X_{MEAN} as well as Y_{MEAN} are in minutes while the location jitters will be specified in terms of % of the wavelength of the power wave. Figs. 2 and 3 show these tilts and jitters.

5. Phase Control System: Since the operation of the spacetenna is retrodirective, it needs a constant phase reference throughout the antenna for conjugator to function properly. This constant phase is supplied to the conjugators by the use of MSRTS in the form of a tree. The master oscillator situated at the physical center of the spacetenna locks onto the phase of the incoming pilot signal. This phase is transmitted to 16 first level slave oscillators, each of these sends the phase to 16 second level slave oscillators. These third level slaves in turn send the phase to 25 fourth level slaves. Fig. 4 shows the phase distribution tree.

Figure 2.

EFFECT OF SUBARRAY TILT

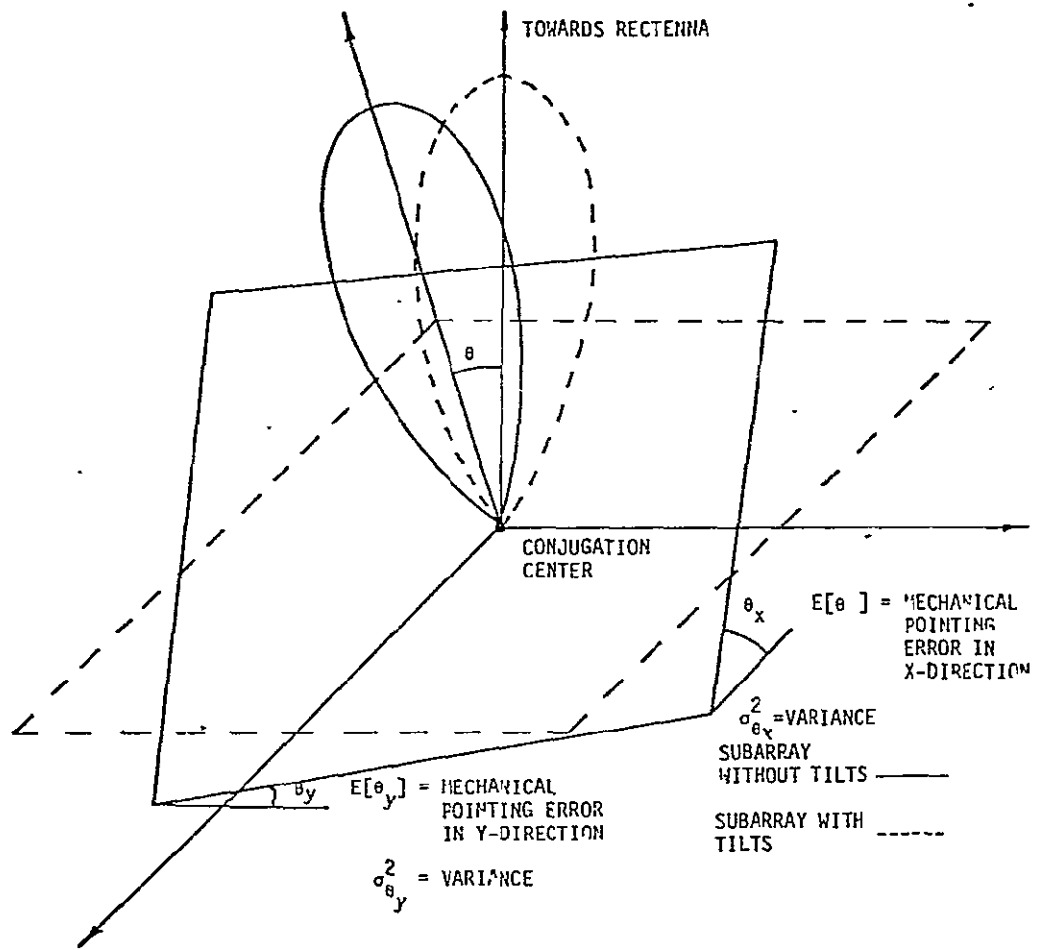
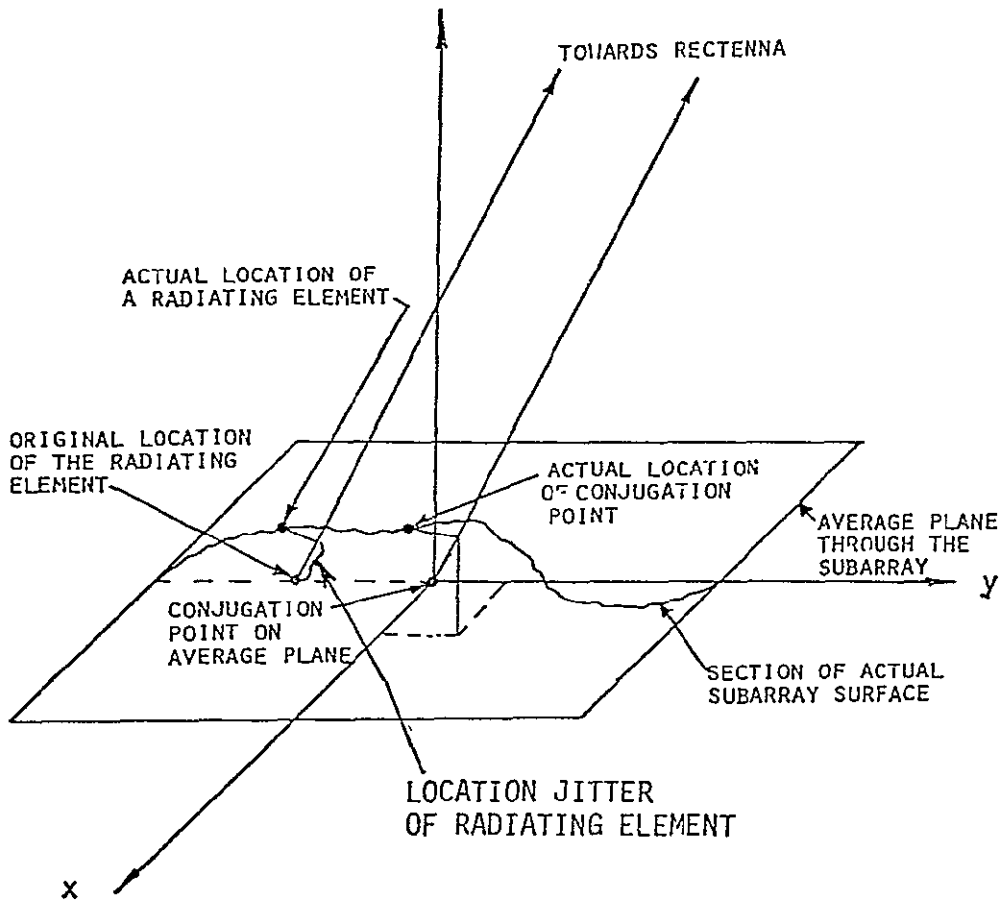
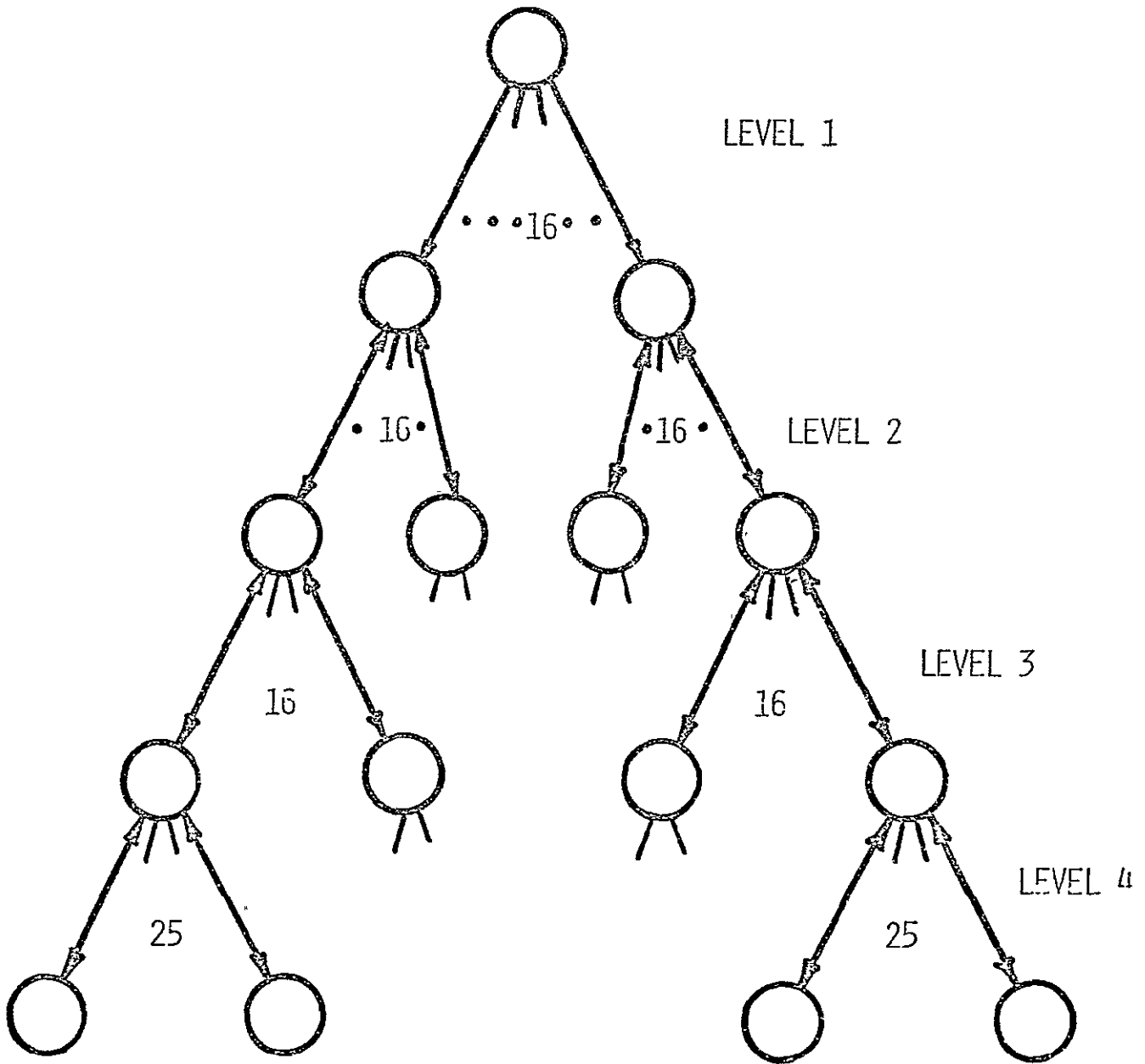


Figure 3.

LOCATION JITTERS OF RADIATING AND RECEIVING ELEMENTS





⊙ PHASE NOISES ARE CORRELATED

⊙ POWER SPLITTERS, POWER TRANSPONDERS, PHASE TRACKING PLLS, MULTIPLIERS, MICROWAVE HARDWARE COMPONENTS

Figure 4. Four Level Phase Distribution Tree.

As the master phase passes from level to level of the phase distribution tree structure it gets corrupted by the phase noise added by the oscillators and the related equipment at each level. The variance of the accumulated noise is designated as SIGMAB(I), I = 1,...,10 for the ten power density circles.

6. Inputs for the Double Integrator Subroutine Supplied by the Computer Library "Math Pack"

The description of these inputs is necessary for the power transfer efficiency program only because a double integration of the averaged power pattern is necessary to obtain the total power radiated by the spacetenna and the power received by the rectenna. The following formula will illustrate the inputs necessary for the program:

$$\text{Power Received on Area 'A'} = \int_{\theta_L}^{\theta_U} \int_{\phi_L}^{\phi_U} \text{APP}(\theta, \phi) \sin \theta d\theta d\phi$$

where APP(θ, ϕ) is the averaged power pattern produced by the spacetenna.

Where

θ_L, θ_U : The lower and upper limits of the variable θ describing the area A.

ϕ_L, ϕ_U : The lower and upper limits of the variable ϕ describing the area A.

Note: To obtain the power received by the rectenna $\theta_L=0$,

$\theta_U = 0.464'$; $\phi_L=0$ and $\phi_U=360^\circ$.

The double integral subroutine approximates the above double integral by the following double sum

$$\int_{\theta_L}^{\theta_U} \int_{\phi_L}^{\phi_U} APP(\theta, \phi) \sin \theta d\theta d\phi \approx \sum_{k=1}^{I_\theta} \sum_{t=1}^{I_\phi} \sum_{i=1}^{N_\theta} \sum_{j=1}^{N_\phi} W_{\theta i} W_{\phi j} APP(\theta_{ki}, \phi_{tj}) \sin \theta_{ki}$$

where

I_θ, I_ϕ : Are the number of intervals on the θ axis and ϕ axis respectively, on the specified θ and ϕ ranges.

N_θ, N_ϕ : Number of points in each of I_θ and I_ϕ respectively in the θ and ϕ ranges.

$W_{\theta i}, W_{\phi j}, \theta_{ki}$ and ϕ_{tj} are generated by the subroutine and does not have to be supplied.

Note: A reasonable input for I_θ, I_ϕ would be 3,3 and for N_θ, N_ϕ would be 4,4.

II. SOLARSIM SUBROUTINE POINTING ERROR

Purpose: SOLARSIM subroutine POINTING ERROR evaluates the effect of phase error introduced by the phase distribution tree (at various levels of the tree) onto the pointing error. It also allows variations in number of levels and number of branches per node at each level of the phase distribution tree.

Inputs: The only necessary inputs are:

Number of levels in the phase distribution tree (PDT)

Number of power density levels

Number of branches per node at each level of PDT

Outputs: The following page shows a sample run of the program.

EXQT

ENTER THE NUMBER OF PHASE DISTRIBUTION TREE LEVELS AND THE NUMBER OF POWER DENSITY LEVELS
>4,10

ENTER THE NUMBER OF BRANCHES PER NODE
>16,16,16,25

ENTER 1 FOR POINTING ERROR FOR SUPPLIED PHASE ERRORS PER LEVEL OF THE PHASE DISTRIBUTION TREE
OR ENTER 2 FOR POINTING ERROR FOR VARIABLE TOTAL RMS PHASE ERROR
>2

ENTER THE STEP SIZE AND NUMBER OF TERMS NECESSARY FOR THE TOTAL RMS PHASE ERROR
IN THE PHASE DISTRIBUTION TREE
>1.0,20

BRANCHING OF THE PHASE DISTRIBUTION TREE:
16 16 16 25

TOTAL RMS PHASE ERROR (DEGREES)	POINTING ERROR (MINUTES)
.00000000	.00000000
1.00000000	.00110421
2.00000000	.00220842
3.00000000	.00331263
4.00000000	.00441683
5.00000000	.00552104
6.00000000	.00662525
7.00000000	.00772946
8.00000000	.00883367
9.00000000	.00993788
10.00000000	.01104209
11.00000000	.01214630
12.00000000	.01325050
13.00000000	.01435471
14.00000000	.01545892
15.00000000	.01656313
16.00000000	.01766734
17.00000000	.01877155
18.00000000	.01987576
19.00000000	.02097996

ENTER 1 FOR A NEW RUN OR 2 TO TERMINATE THE RUN
>2

III. SOLARSIM SUBROUTINE VARSUB

Purpose: SOLARSIM subroutine VARSUB evaluates the effect of various tilts of the subarrays, the location jitters of the power radiating and pilot receiving elements and finally the phase distribution system errors on the gain of the spacetenna.

Inputs:

CURNT(I)	I = 1, ..., 10
N(I)	I = 1, ..., 10
M(I)	I = 1, ..., 10
SIGPSI(I)	I = 1, ..., 10
SIGPHI(I)	I = 1, ..., 10
SIGMAB(I)	I = 1, ..., 10
YMEAN(I)	I = 1, ..., 10
XMEAN MAX	Maximum XMEAN tilt in minutes
SIGMA(I)	I = 1, 2, ..., 10

Note that this program does need the integrator subroutine to generalize the weights. Figure 5 is the flow chart of the program.

Output: The output is plotted in Figure 6.

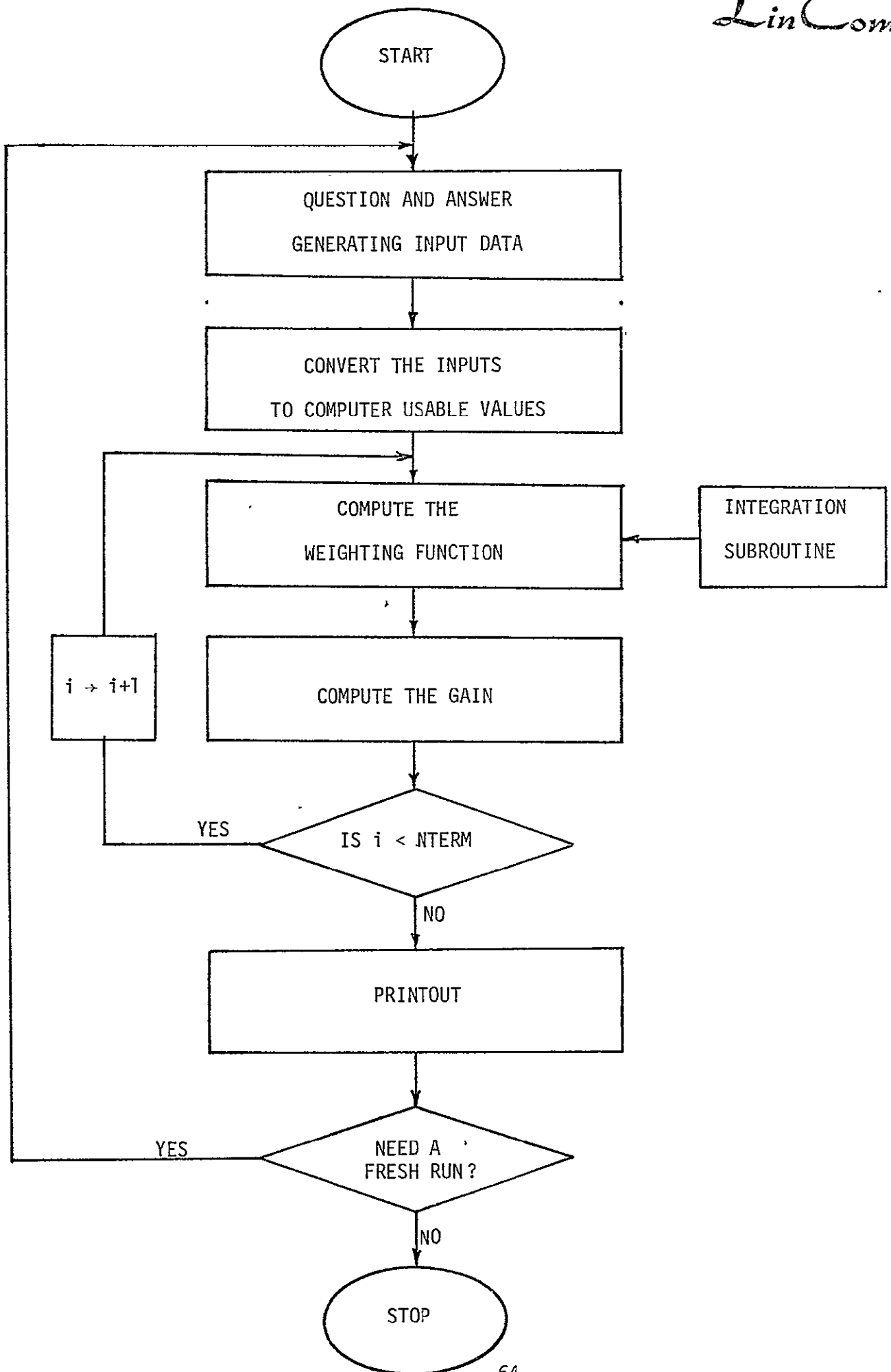


Figure 5.

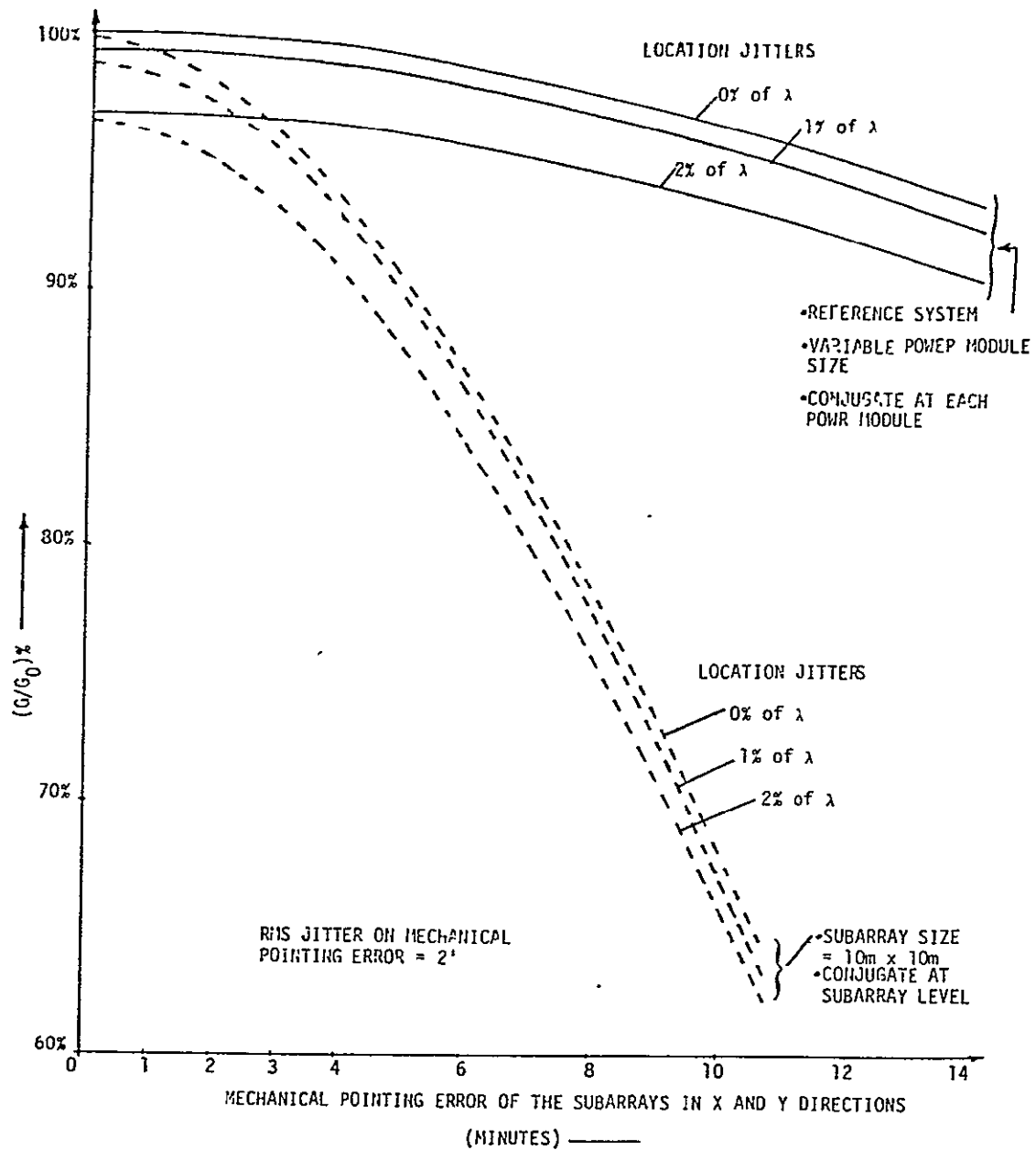


Figure 6. Sensitivity to Tilt Effects as a Function of Phase Conjugation Level.

Sample Run for Subroutine VARSUB:

@XQT EXFILE

INPUTS FOR THE TILT PROGRAM BEGIN

PRINT 1 FOR USING THE BASELINE CURRENT TAPER OR 2 FOR DIFFERENT TAPER
>1

ENTER 1 FOR USING BASELINE FOR NUMBER OF SLOTS PER POWER RING OR 2 FOR DIFFERENT NUMBER OF SLOTS
>1

ENTER 1 FOR USING BASELINE FOR NUMBR OF SLOTS PER SUBARRAY IN EACH POWER RING OR 2 FOR DIFFERENT NUMBER OF SLOTS
>1

ENTER 1 FOR SAME LOCATION JITTERS ON THE RADIATING ELEMENTS IN ALL POWER RINGS OTHERWISE ENTER 2
>1

ENTER THE COMMON LOCATION JITTER OF THE RADIATING ELEMENTS IN TERMS OF % OF LAMBDA
>0.0

ENTER 1 FOR SAME LOCATION JITTER ON THE CONJUGATION POINT IN ALL POWER RINGS OTHERWISE ENTER 2
>1

ENTER COMMON LOCATION JITTER FOR THE CONJIGATION POINT
>0.0

ENTER 1 FOR SAME X AND Y TILTS FOR SUBARRAYS OTHERWISE ENTER 2
>1

ENTER THE MAXIMUM TILT FOR X AND Y DIRECTIONS
>20.0

ENTER 1 FOR SAME TILT JITTER FOR EACH POWER RING OTHERWISE ENTER 2
>1

ENTER THE COMMON JITTERS ON TILTS
>2.0

ENTER THE NUMBER OF POINTS DESIRED ON X AXIS
>20

INPUTS FOR TILT PROGRAM COMPLETE

X&Y TILT (MINUTES)	(G/G0) %	G/G0 IN DB
.00000000	99.85770130	-.00618432
.99999433	99.82218361	-.00772931
1.99998876	99.71570778	-.01236422
2.99998331	99.53852844	-.02008782
3.99997815	99.29104519	-.03009910
4.99997330	98.97384453	-.04479558
5.99996895	98.58765316	-.06177469
6.99996501	98.13335609	-.08183345
7.99996173	97.61200237	-.10496774
8.99995911	97.02478409	-.13117314
9.99995720	96.37302971	-.16044484
10.99995625	95.65822220	-.19277693
11.99995625	94.80196564	-.22816325
12.99995708	94.04599380	-.26659697
13.99995911	93.15216064	-.30807066
14.99996233	92.20243931	-.35257586
15.99996606	91.19889355	-.40010427
16.99997234	90.14369488	-.45064642
17.99997997	89.03910637	-.50419205
18.99998856	87.88746357	-.56073068

ENTER 1 FOR FRESH RUN OR 2 FOR TERMINATION

IV. SOLARSIM SUBROUTINE POWER PATTERN:

Purpose: The purpose of this subroutine is to study the effects of parameters like the subarray tilts, the phase jitters, current amplitude jitter, etc. on the power pattern produced by the spaceteenna.

Inputs:

N(I) I = 1, ..., 10

M(I) I = 1, ..., 10

NA(I) I = 1, ..., 10

R(I) I = 1, ..., 10

SIGMAB(I) I = 1, ..., 10

SIGPSI(I) I = 1, ..., 10

SIGPHI(I) I = 1, ..., 10

SIGMAI(I) I = 1, ..., 10

CURNT(I) I = 1, ..., 10

XMEAN(I) I = 1, ..., 10

SIGMA(I) I = 1, ..., 10

PHI The value of ϕ direction in which the pattern is generated.

Figure 7 depicts the flow chart for this program.

Output: With the plot option incorporated, the output is shown in Figure 8. Here the pattern is for RMS phase error of 10° mechanical pointing error of $4'$ and the jitter on mechanical pointing error = $2'$ and the location jitters of 4%.

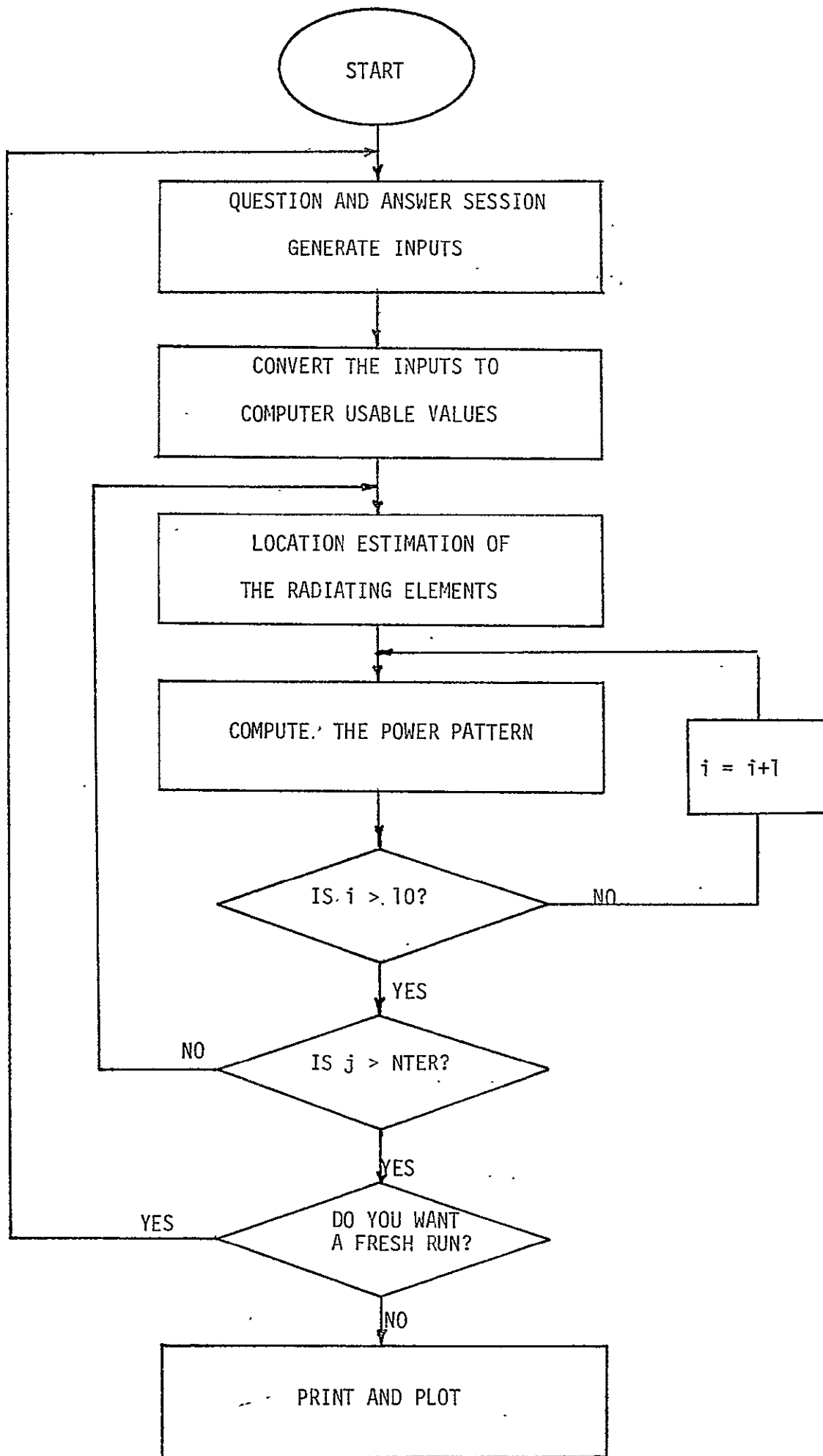


Figure 7.

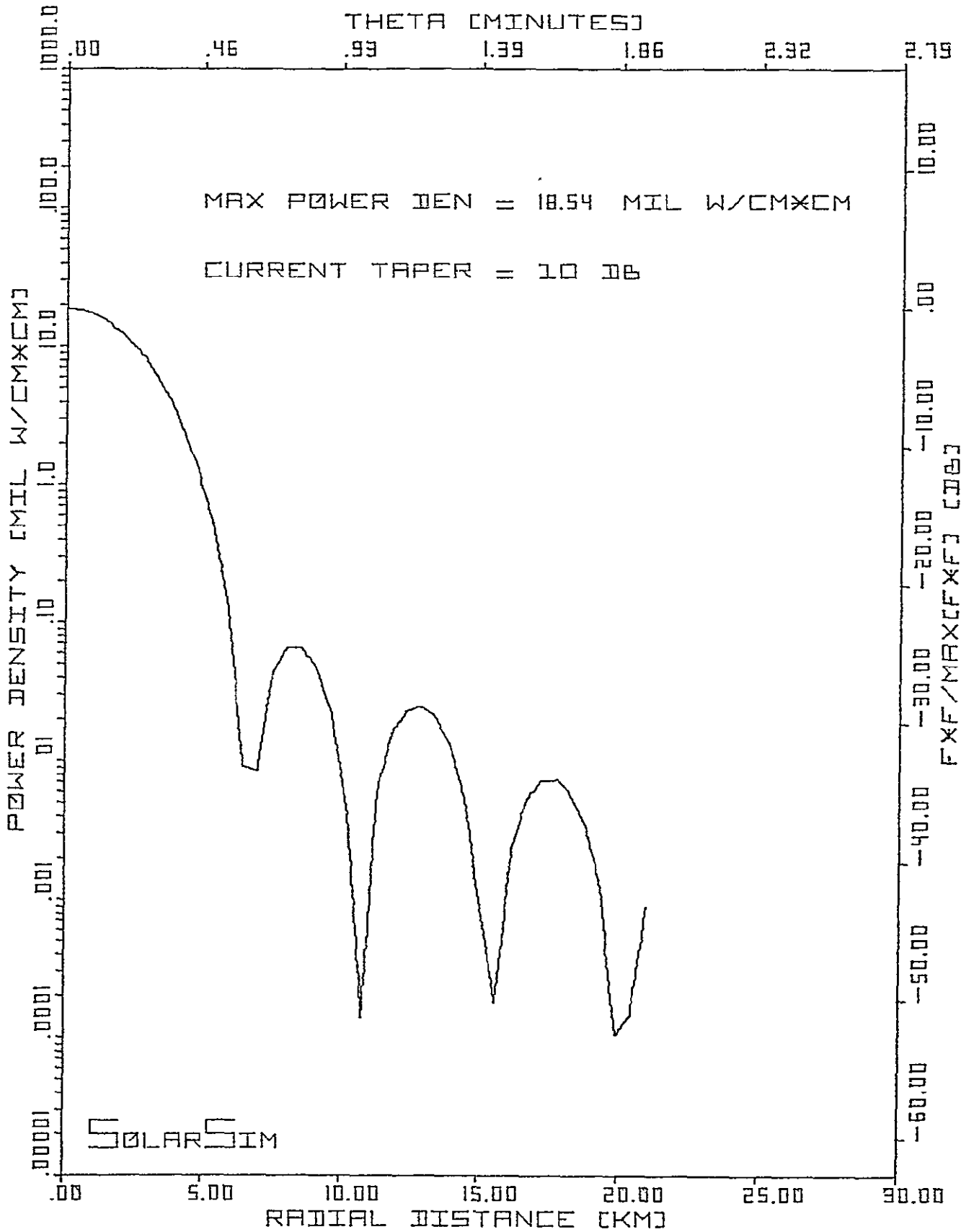


Figure 8. A Typical Power Pattern with Nonzero Tilts and Jitters.

V. SOLARSIM SUBROUTINE POWER TRANSFER EFFICIENCY

Purpose: The purpose of SOLARSIM subroutine power transfer efficiency is to study the effects of perturbations, mechanical or otherwise, on the power transfer efficiency of the spacenna. It also has provision to investigate the changes produced in the power pattern due to the above mentioned perturbations.

Inputs: The program has an extensive question and answer session generating all the necessary inputs. The following quantities are needed for this program.

N(I) I = 1,.....,N

M(I) I = 1,.....,N

NA(I) I = 1,.....,N

R(I) I = 1,.....,N

SIGMAB(I) I = 1,.....,N

SIGPSI(I) I = 1,.....,N

SIGPHI(I) I = 1,.....,N

SIGMAI(I) I = 1,.....,N

CURNT(I) I = 1,.....,N

XMEAN(I) I = 1,.....,N

SIGMA(I) I = 1,.....,N

(θ_r, ϕ_r)

All the above inputs are necessary for either the power transfer efficiency or the power pattern computations. If you desire the power pattern output then the following additional inputs are necessary:

PHI value of ϕ direction in which the pattern is generated.

NTERM The number of θ value at which the pattern will
be evaluated.

STEP The step size for θ evaluation.

If you desire the power transfer efficiency of the spacetenna, the following additional inputs will be necessary.

Xa,Xb Lower and upper limits of theta integration in
minutes..

Ya,Yb Lower and upper limits of phi integration in
degrees.

Nx,Ny Number of points to be used per interval in the
Gauss Quadrature approximation of the integral

Ix,Iy Number of intervals in the theta and phi range to
be considered for the integration.

Outputs: There is no plot option available yet hence a hand plotted version of the printed output is shown in Figure 10. The solid as well as the dashed lines here generated by using the efficiency program.

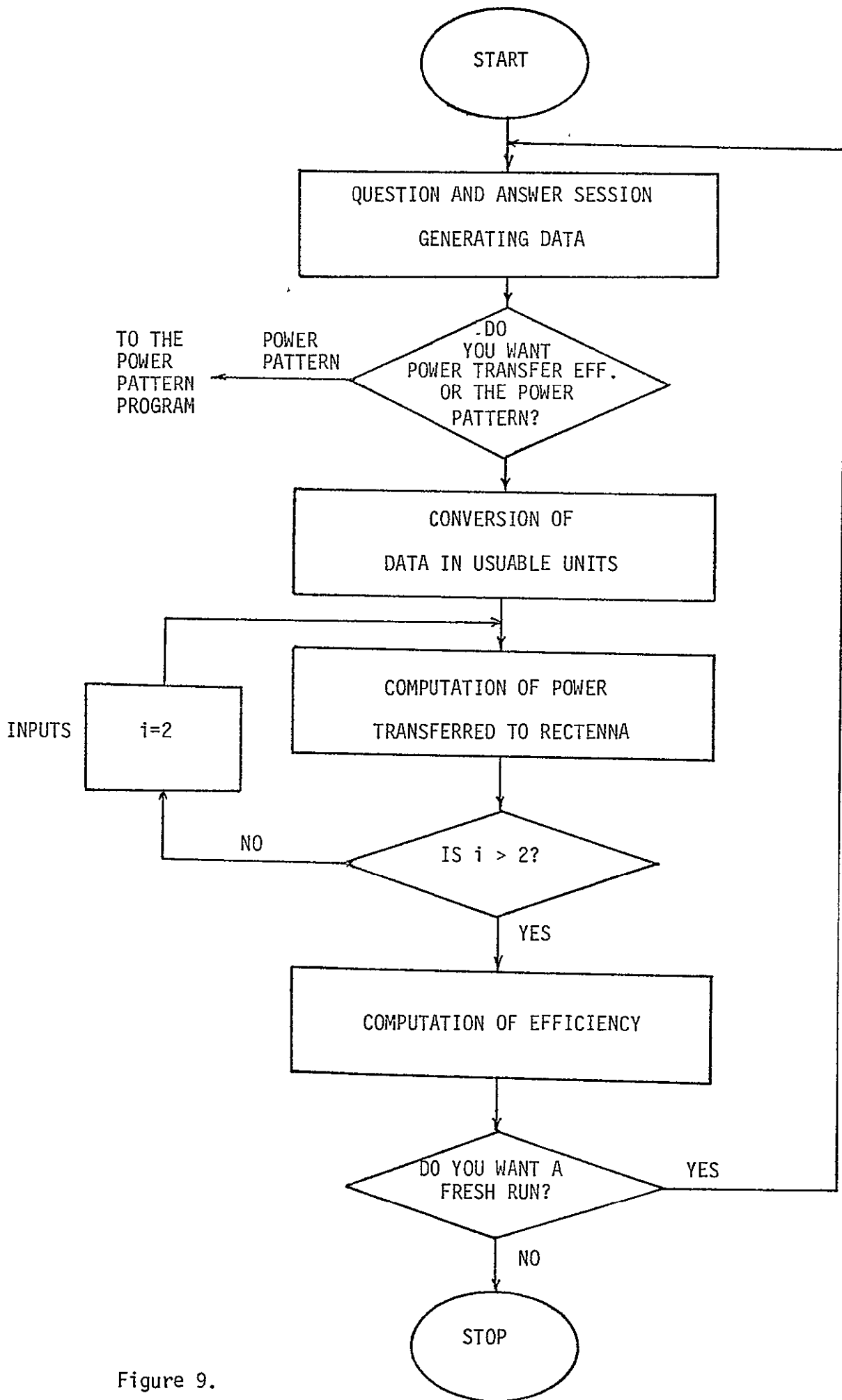
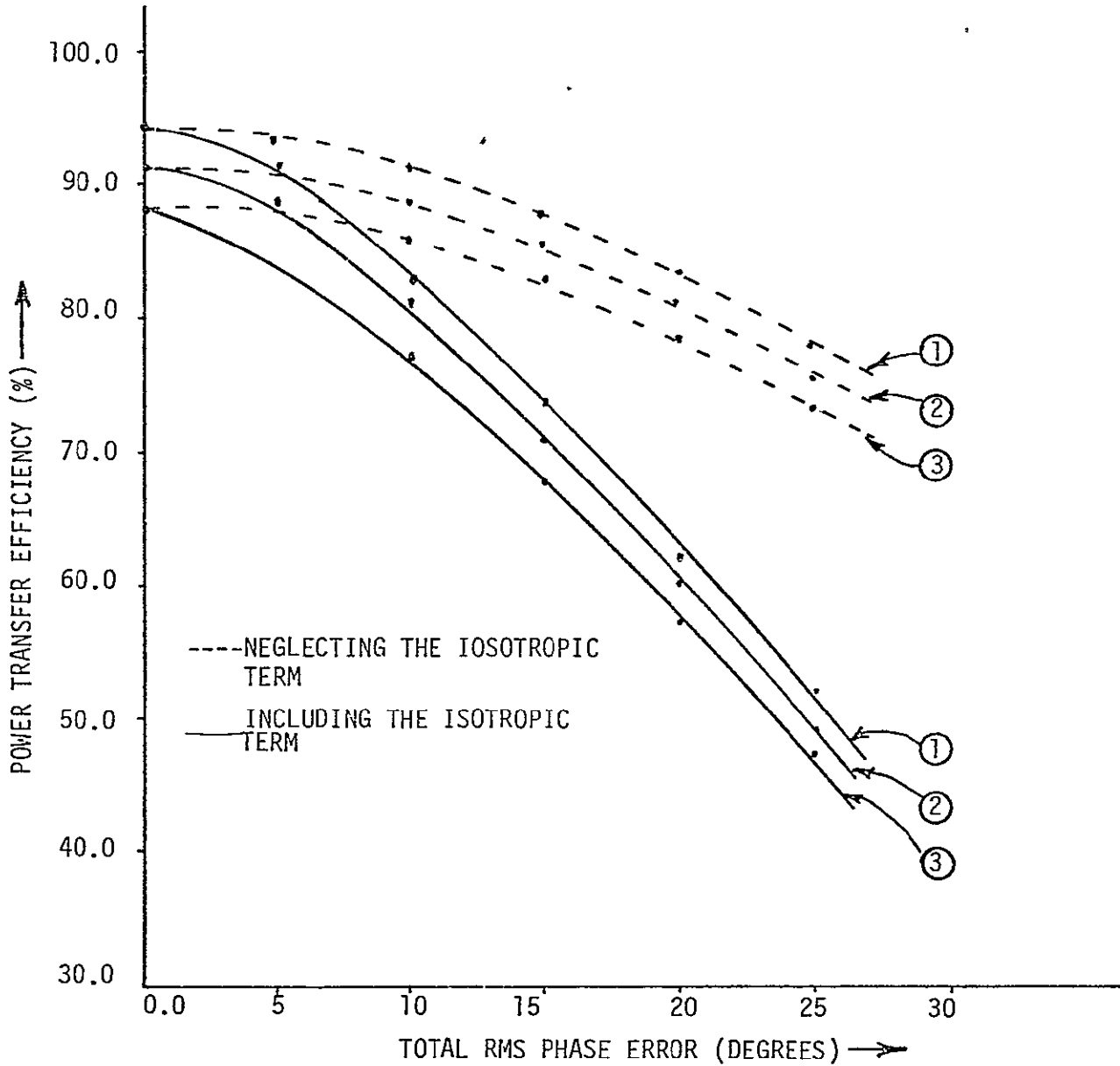


Figure 9.

CURRENT TAPER 10 dB



LEGEND

- ① MECHANICAL POINTING ERROR (MPE) = 0, LOCATION JITTERS (LJ) = 0, JITTER ON MECHANICAL POINTING = 0
- ② MPE 10', LJ = 0, JITTER ON MPE = 2'
- ③ MPE = 10', LJ = 2% of λ , JITTER ON MPE = 2'

Figure 10.

Sample Runs:

The power transfer efficiency program is run for two different sets of inputs:

- (1) The case when the location jitters on the radiating and receiving elements as well as the current amplitude jitters are constants for the spacetenna, i.e., they do not change from power ring to power ring. In such a case the program has the capability of looping back and changing the initial conditions of the parameters. The program is run for different initial conditions for the parameters.
 - (i) Any one of the parameters is allowed to vary producing a set of values for the efficiency holding all the other parameters to constant values.

@XQT EXFILE

ENTER APP FOR THE AVERAGED POWER PATTERN OR PTE FOR POWER TRANSFER EFFICIENCY:
>PTE

INPUTS FOR THE EFFICIENCY PROGRAM BEGIN:

ALL THE FOLLOWING QUESTIONS SHOULD BE ANSWERED IN YES OR NO OR GIVE THE DATA:

DO YOU WANT BASELINE NUMBER OF POWER DENSITY STEP?
>YES

DO YOU WANT THE BASELINE CURRENT TAPER?
>YES

DO YOU WANT THE BASELINE NUMBER OF SLOTS PER POWER RING?
>YES

DO YOU WANT BASELINE NUMBER OF SLOTS PER SUBARRAY IN EACH POWER RING?
>YES

DO YOU WANT THE SAME LOCATION JITTER ON THE RADIATING ELEMENTS IN ALL POWER RINGS?
>YES

ENTER THE COMMON LOCATION JITTER OF THE RADIATING ELEMENTS IN TERMS OF % OF LAMBDA:
>0.0

DO YOU WANT THE SAME LOCATION JITTERS ON THE CONJUGATION POINTS IN ALL THE POWER RINGS?
>YES

ENTER THE COMMON LOCATION JITTER OF THE CONJUGATION POINTS IN ALL THE POWER RINGS IN % OF LAMBDA:
>0.0

IN EACH POWER RING THE MEAN X AND MEAN Y TILTS WILL BE ASSUMED SAME:

DO YOU WANT SAME MEAN VALUES FOR X AND Y TILTS IN DIFFERENT POWER DENSITY RINGS?
>YES

ENTER THE COMMON MEAN X AND Y TILTS IN MINUTES:
>0.0

DO YOU WANT SAME TILT JITTERS FOR THE IN ALL POWER RINGS?
>YES

ENTER THE COMMON TILT JITTERS ON ALL SUBARRAYS IN THE SPACETENNA:
>0.0

ENTER THE NUMBER OF INTERVALS TO BE CONSIDERED FOR THE THETA RANGE:

>6

.00000000

84914732.00000000 3519558.62500000
88434290.00000000

81940746.00000000 7940756.18750000
89881502.00000000

-81940732.00000000 -7940755.12500000
-89881487.00000000

14.87500000

88434304.00000000

IN WHAT FOLLOWS ENTER ONLY ONE NUMBER DIFFERENT FROM 1 EXCEPTING THAT ALL THE NUMBERS SHOULD BE EQUAL TO 0 TO STOP THE RUN

ENTER THE NUMBER OF PHASE JITTERS, NUMBER OF LOCATION JITTERS ON RADIATING ELEMENTS NUMBER OF LOCATION JITTERS ON RECEIVING ELEMENTS AND THE NUMBER OF AMPLITUDE JITTERS

>15,1,1,1

DO YOU WANT TO CHANGE THE INITIAL CONDITIONS LOCATION JITTERS ON TRANSMITTING AND RECEIVING ELEMENTS, AMPLITUDE JITTERS AND THE PHASE JITTERS?

>YES

ENTER THE INITIAL CONDITIONS FOR ALL THE PARAMETER IN THE ORDER: LOCATION JITTERS ON TRANSMITTING ELEMENTS, LOCATION JITTERS ON RECEIVING ELEMENTS, AMPLITUDE JITTERS AND THE PHASE JITTERS.
THE SELECTED VARIABLE

>0.0,0.0,0.0

ENTER THE STARTING POINT AND STEP OF THE VARIABLE

>0.0,1.0

LOCATION JITTERS ON THE RADIATING ELEMENTS (% OF LAMBDA) = .00000
LOCATION JITTERS ON THE RECEIVING ELEMENTS (% OF LAMBDA) = .00000
AMPLITUDE JITTERS (PERCENT) = .00000

TOTAL PHASE ERROR (DEGREES)	POWER TRANSFER EFFICIENCY (PERCENT)
.000000	92.567389
1.000000	92.435296
2.000000	92.451071
3.000000	92.310868

4.000000	92.114939
5.000000	91.863640
6.000000	91.557421
7.000000	91.196837
8.000000	90.782539
9.000000	90.315270
10.000000	89.795861
11.000000	89.225241
12.000000	88.604421
13.000000	87.934499
14.000000	87.216649

IN WHAT FOLLOWS ENTER ONLY ONE NUMBER DIFFERENT FROM 1 EXCEPTING THAT ALL THE NUMBERS SHOULD BE EQUAL TO 0 TO STOP THE RUN

ENTER THE NUMBER OF PHASE JITTERS, NUMBER OF LOCATION JITTERS ON TRANSMITTING ELEMENTS, NUMBER OF LOCATION JITTERS ON RECEIVING ELEMENTS AND THE NUMBER OF AMPLITUDE JITTERS
>1,15,1,1

DO YOU WANT TO CHANGE THE INITIAL CONDITIONS LOCATION JITTERS ON TRANSMITTING AND RECEIVING ELEMENTS, AMPLITUDE JITTERS AND THE PHASE JITTERS?
>YES

ENTER THE INITIAL CONDITIONS FOR ALL THE PARAMETER IN THE ORDER: LOCATION JITTERS ON TRANSMITTING ELEMENTS, LOCATION JITTERS ON RECEIVING ELEMENTS, AMPLITUDE JITTERS AND THE PHASE JITTERS.
THE SELECTED VARIABLE
>0.0,0.0,0.0

ENTER THE STARTING POINT AND STEP OF THE VARIABLE
>0.0,1.0

LOCATION JITTERS ON RECEIVING ELEMENTS (% OF LAMBDA) = .00000
AMPLITUDE JITTER (PERCENT) = .00000
PHASE JITTER (DEGREES) = .00000

LOCATION JITTERS ON RADIATING ELEMENTS (% OF LAMBDA)	POWER TRANSFER EFFICIENCY (PERCENT)
.000000	92.63389
1.000000	91.490627
2.000000	88.392965
3.000000	83.600305
4.000000	77.70030
5.000000	70.795266
6.000000	63.718729
7.000000	56.695977
8.000000	49.78714
9.000000	43.724494
10.000000	38.015780
11.000000	32.880841
12.000000	28.312103
13.000000	24.280330
14.000000	20.744736

IN WHAT FOLLOWS ENTER ONLY ONE NUMBER DIFFERENT FROM 1 EXCEPTING THAT ALL THE NUMBERS SHOULD BE EQUAL TO 0 TO STOP THE RUN

ORIGINAL PAGE IS
OF POOR QUALITY

ENTER THE NUMBER OF PHASE JITTERS,NUMBER OF LOCATION JITTERS ON RADIATING ELEMENTS NUMBER OF LOCATION JITTERS ON RECEIVING ELEMENTS AND THE NUMBER OF AMPLITUDE JITTERS
>1,1,15,1

DO YOU WANT TO CHANGE THE INITIAL CONDITIONS LOCATION JITTERS ON TRANSMITTING AND RECEIVING ELEMENTS,AMPLITUDE JITTERS AND THE PHASE JITTERS?
>YES

ENTER THE INITIAL CONDITIONS FOR ALL THE PARAMETER IN THE ORDER: LOCATION JITTERS ON TRANSMITTING ELEMENTS, LOCATION JITTERS ON RECEIVING ELEMENTS,AMPLITUDE JITTERS AND THE PHASE JITTERS DELETING THE SELECTED VARIABLE
>0.0,0.0,0.0

ENTER THE STARTING POINT AND STEP OF THE VARIABLE
>0.0,1.0

LOCATION JITTERS ON RADIATING ELEMENTS (% OF LAMBDA) = .00000
AMPLITUDE JITTERS (PERCENT) = .00000
PHASE JITTER (DEGREES) = .00000

LOCATION JITTERS ON RECEIVING ELEMENTS (% LAMBDA)	POWER TRANSFER EFFICIENCY(PERCENT)
.000000	92.63389
1.000000	92.199979
2.000000	91.118254
3.000000	89.343413
4.000000	86.916371
5.000000	83.892200
6.000000	80.330070
7.000000	76.330790
8.000000	71.754062
9.000000	67.295571
10.000000	62.444160
11.000000	57.407029
12.000000	52.507244
13.000000	47.501551
14.000000	42.770620

IN WHAT FOLLOWS ENTER ONLY ONE NUMBER DIFFERENT FROM 1 EXCEPTIN- THAT ALL THE NUMBERS SHOULD BE EQUAL TO 0 TO STOP THE RUN

ENTER THE NUMBER OF PHASE JITTERS,NUMBER OF LOCATION JITTERS ON RADIATING ELEMENTS NUMBER OF LOCATION JITTERS ON RECEIVING ELEMENTS AND THE NUMBER OF AMPLITUDE JITTERS
>1,1,1,15

DO YOU WANT TO CHANGE THE INITIAL CONDITIONS LOCATION JITTERS ON TRANSMITTING AND RECEIVING ELEMENTS,AMPLITUDE JITTERS AND THE PHASE JITTERS?
>YES

ENTER THE INITIAL CONDITIONS FOR ALL THE PARAMETER IN THE ORDER: LOCATION JITTERS ON TRANSMITTING ELEMENTS, LOCATION JITTERS ON RECEIVING ELEMENTS,AMPLITUDE JITTERS AND THE PHASE JITTERS.DELETING THE SELECTED VARIABLE.

ENTER THE STARTING POINT AND STEP OF THE VARIABLE
>0.0,1.0

LOCATION JITTERS ON RADIATING ELEMENTS (% OF LAMBDA) = .00000
LOCATION JITTERS ON RECEIVING ELEMENTS % OF LAMBDA) = .00000
PHASE JITTER (DEGREES) = .00000

AMPLITUDE JITTERS ON CURRENTS	POWER TRANSFER EFFICIENCY (PERCENT)
.000000	92.563389
1.000000	92.554169
2.000000	92.526510
3.000000	92.488454
4.000000	92.416051
5.000000	92.333378
6.000000	92.232536
7.000000	92.113642
8.000000	91.976836
9.000000	91.822280
10.000000	91.658155
11.000000	91.468659
12.000000	91.254016
13.000000	91.030458
14.000000	90.798244

>IN WHAT FOLLOWS ENTER ONLY ONE NUMBER DIFFERENT FROM 1 EXCEPTING THAT ALL THE NUMBERS SHOULD BE EQUAL TO 0 TO STOP THE RUN

ENTER THE NUMBER OF PHASE JITTERS, NUMBER OF LOCATION JITTERS ON RADIATING ELEMENTS NUMBER OF LOCATION JITTERS ON RECEIVING ELEMENTS AND THE NUMBER OF AMPLITUDE JITTERS
>0,0,0,0

CPU TIME USED (MINUTES) =4.84651661

DO YOU WANT A FRESH RUN?

>NO

- (2) The case when either the location jitters on the transmitting elements or the location jitters on the receiving elements or the current amplitude jitters are different for different power raings then the program does not loop back and produces only one efficiency for one set of conditions.

(b)

EXQT EXFILE

ENTER APP FOR THE AVERAGED POWER PATTERN OR PTE FOR POWER TRANSFER EFFICIENCY:
>PTC

INPUTS FOR THE EFFICIENCY PROGRAM BEGIN:

ALL THE FOLLOWING QUESTIONS SHOULD BE ANSWERED IN YES OR NO OR GIVE THE DATA:

DO YOU WANT BASELINE NUMBER OF POWER DENSITY STEP?
>YES

DO YOU WANT THE BASELINE CURRENT TAPER-
>YES

DO YOU WANT THE BASELINE NUMBER OF SLOTS PER POWER RING?
>YES

DO YOU WANT BASELINE NUMBER OF SLOTS PER SUBARRAY IN EACH POWER RING?
>YES

DO YOU WANT THE SAME LOCATION JITTER ON THE RADIATING ELEMENTS IN ALL POWER RINGS?
>NO

ENTER THE LOCATION JITTERS OF THE RADIATING ELEMENTS IN % OF LAMBDA FOR EACH POWER RING:
>1.0,2.0,3.0,4.0,5.0,6.0,7.0,8.0,9.0,10.0

DO YOU WANT THE SAME LOCATION JITTERS ON THE CONJUGATION POINTS IN ALL THE POWER RINGS?
>YES

ENTER THE COMMON LOCATION JITTER OF THE CONJUGATION POINTS IN ALL THE POWER RINGS IN % OF LAMBDA:
>0.0

IN EACH POWER RING THE MEAN X AND MEAN Y TILTS WILL BE ASSUMED SAME:

DO YOU WANT SAME MEAN VALUES FOR X AND Y TILTS IN DIFFERENT POWER DENSITY RINGS?
>YES

ENTER THE COMMON MEAN X AND Y TILTS IN MINUTES.
>10.0

DO YOU WANT SAME TILT JITTERS FOR THE IN ALL POWER RINGS?
>YES

ENTER THE COMMON TILT JITTERS ON ALL SUBARRAYS IN THE SPACETENNA:
>2.0

ENTER THE NUMBER OF INTERVALS TO BE CONSIDERED FOR THE THETA RANGE
>6

24843751.00000000

73164039.00000000 2831029.46875000
75995068.00000000

7179421.07500000 789378.24210750
7968000.06250000

-6938512.01250000 -762197.04687500
-7700709.01250000

268090.20312500

101107709.00000000
POWER TRANSFER EFFICIENCY (PERCENT) = 78.86430

CPU TIME USED (MINUTES) = 5.40486664.

DO YOU WANT A FRESH RUN-
>NO